Journal of Geochemical Exploration 232 (2022) 106700

Contents lists available at ScienceDirect

Journal of Geochemical Exploration

journal homepage: www.elsevier.com/locate/gexplo

Tungsten skarn potential of the Yukon-Tanana Upland, eastern Alaska, USA—A mineral resource assessment

George N.D. Case [a,*], Garth E. Graham [b], Erin E. Marsh [b], Ryan D. Taylor [b], Carlin J. Green [c], Philip J. Brown [b], Keith A. Labay [a]

[a] U.S. Geological Survey, Alaska Science Center, Anchorage, AK 99508, USA
[b] U.S. Geological Survey, Geology, Geophysics and Geochemistry Science Center, CO 80225, USA
[c] U.S. Geological Survey, Geology, Energy and Minerals Science Center, Reston, VA 20192, USA

ARTICLE INFO

Keywords:
Mineral resource assessment
Tungsten
Critical mineral
Mineral potential mapping
Alaska

ABSTRACT

Tungsten (W) is used in a variety of industrial and technological applications and has been identified as a critical mineral for the United States, India, the European Union, and other countries. These countries rely on W imports mostly from China, which leaves them vulnerable to supply disruption. Consequently, the U.S. government has a current initiative to understand domestic resource potential. The eastern Alaska portion of the Yukon-Tanana Upland (YTU), is prospective for W skarn deposits, the major source of global W supply. The regional geology consists of juxtaposed Paleozoic lithotectonic packages that were reaccreted to North America in the Mesozoic. Multiple subsequent episodes of arc-related magmatism intruded the lithotectonic packages, accompanied by W skarn formation mostly associated with 100–90 Ma intrusions; major W skarn deposits in Canada are part of the same metallogenic event (e.g., Mactung, Cantung). In this paper, we present an assessment for undiscovered W skarn resources for parts of the lesser-explored western (Alaskan) portion of the YTU.

We used GIS proximity analysis to map the intersection of pluton and carbonate-bearing rocks to define three permissive tracts for W skarn deposits. The permissive tracts were qualitatively assessed by mineral potential mapping using region-wide sediment geochemistry and mineral concentrate datasets. This analysis showed that much of the western YTU has high potential for undiscovered W skarn deposits, whereas the eastern and southern YTU had only isolated areas of medium to high potential. Historical production and the quality of the geochemistry data of the western YTU tract (ca. 9200 km^2) permitted a quantitative assessment of undiscovered W resources. Probabilistic estimates by a panel of 20 experts predicted a 70% chance of one to three undiscovered W skarn deposits in the western YTU tract. The rationale for favorability employed by the expert panel included favorable lithology, previous production, clustering of previously mined deposits, W placers in the area, lack of recent exploration, pan concentrates containing W minerals, and W geochemical anomalies. Estimates were combined with a global grade and tonnage model for W skarns in a Monte Carlo simulation and provided a median estimate of undiscovered resources of 94 kt WO_3. If the undiscovered W skarn deposits are located close to infrastructure (e.g., near Fairbanks, or close to roads and/or power grid), application of an economic filter indicates that the median total economically recoverable WO_3 is 63 kt with a net present value (NPV) of $330 million USD (2008 dollars). Whereas if deposits are far from infrastructure, median recoverable WO_3 is only 30 kt and the NPV is $44 million.

Our models for contained WO_3 resources and NPV estimates for the western YTU tract are considerably lower than the known resources in skarns in adjacent areas in Canada. Estimates for the western YTU are also lower than preliminary estimates for undiscovered W skarn deposits in areas of the western conterminous United States. We speculate that lower permeability and continuity of favorable carbonate rock horizons in the relatively higher-grade metamorphic country rocks in the Alaska portion of the YTU may explain some of the differences in prospectivity. More detailed geologic mapping, modern geochemistry, and geophysical surveys are needed to refine the resource potential of the whole YTU. Regardless, quantitative mineral resource assessment provides a useful tool for making first-order regional estimates of undiscovered resources, identifying target areas for new data acquisition, and guiding research on the fundamental controls of district-scale metallogenic endowments.

* Corresponding author.
E-mail address: gcase@usgs.gov (G.N.D. Case).

https://doi.org/10.1016/j.gexplo.2020.106700
Received 9 May 2020; Received in revised form 31 October 2020; Accepted 22 November 2020
Available online 25 November 2020

1. Introduction

Tungsten (W) is one of the hardest metals, has the highest melting point of any pure metal, and is an important alloying agent. It is used in the aerospace, defense, energy, and telecommunications and electronics sectors. Notable applications include jet engines, catalysts, filaments, and cutting and drilling tools. Nearly 60% of W used in the United States is for cemented carbide parts for industrial use in wear-resistant applications (U.S. Geological Survey, 2020a).

The U.S. Government recently classified W as one of 35 non-fuel critical minerals and elements that are strategically important because of reliance on imports, relative scarcity, and importance to economic and national security (Fortier et al., 2018). Other large countries and organizations, including India and the European Union, have also identified W as a critical mineral (Gupta et al., 2016; Deloitte Sustainability et al., 2017).

Tungsten is one of the few commodities on the U.S. critical minerals list that can be mined as a primary commodity even despite its average crustal abundance relative to other critical commodities. For comparison, W is approximately 20 to 50 times less abundant than the rare earth elements lanthanum and cerium (~1.4 ppm W and 31.7 ppm La; Hu and Gao, 2008; ~64 ppm Ce; Taylor and McLennan, 1985). Despite its importance in technology and aerospace applications, no primary W has been produced in the United States since 2016. China produced over 80% of the world's supply of W in both 2017 and 2018. In 2019, China accounted for 70 kt of the 85 kt of W produced globally (approximately 82.4%), far eclipsing the next two largest producers (Vietnam at 4.8 kt (5.6%) and Mongolia at 1.9 kt (2.2%); U.S. Geological Survey, 2020a).

Several deposit types can host economic W (e.g., Cox and Singer, 1986); the most commonly exploited W deposit types include skarn, vein, and greisen deposits (e.g., British Geological Survey, 2011). Historically, however, >70% of the world's W has been mined from skarn

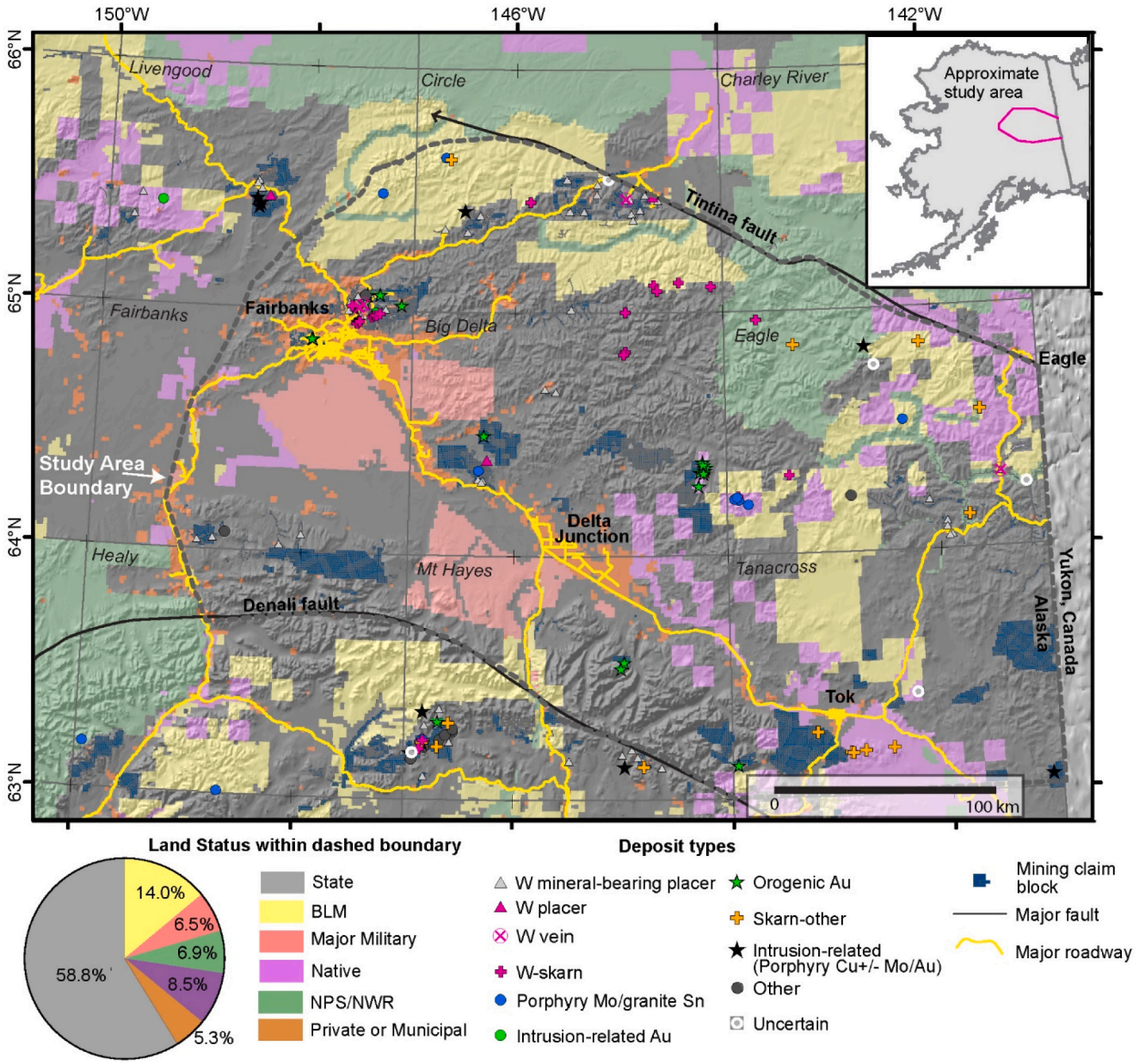

Fig. 1. Study area location map. Shaded areas represent land status and claim blocks. Occurrence symbols represent various deposit and occurrence types in the study area (Alaska Resource Data File; https://ardf.wr.usgs.gov/index.php). BLM – Bureau of Land Management, NPS – National Park Service, NWR – National Wildlife Refuge.

deposits (Misra, 2000). Tungsten skarns are known on every continent except Antarctica. Notable deposits include King Island, Australia; Sang Dong, South Korea; Los Santos, Spain; Shizhuyuan, China; Vostok-2, Russia; and Bonfirm and Brejui, Brazil (Green et al., 2020). In North America, significant deposits include Pine Creek, California, United States, and the Cantung and Mactung deposits, in Northwest Territories and Yukon, Canada, respectively (Green et al., 2020).

In this contribution, we provide an assessment for W skarn resources of an 120,000 km^2 area of Alaska. The region extends from west of Fairbanks to the Canadian border and is bounded by the Tintina and Denali faults on the north and south, respectively (Fig. 1). Historical W production from skarn deposits was restricted to the Fairbanks area (~3.57 kt of WO_3; Nokleberg et al., 1987); however, because parts of this region have grossly similar geology to the Cantung and Mactung deposit areas, potential for additional resources exists. Prior to this assessment, the Circle quadrangle (Fig. 1) was the only area assessed for W skarn (and Sn greisen) potential in this region (Menzie et al., 1983). Other reports have characterized known mineral occurrences but did not assess for undiscovered W deposits (e.g., Menzie and Foster, 1978; U.S. Bureau of Mines, 1995).

This assessment incorporates the U.S. Geological Survey (USGS) three-part methodology (Singer and Menzie, 2010), integrating existing geologic and geochemical data, expert knowledge, a new grade and tonnage model (Green et al., 2020), and new economic filters (Shapiro and Robinson, 2019). The results and geologic implications of this assessment are compared to known endowments and other assessments of undiscovered W skarn resources elsewhere in the North American Cordillera.

2. An overview of W-Skarn deposits

2.1. Deposit model

Deposits formed in the magmatic-hydrothermal mineral system environment account for most global hardrock tungsten production. This environment encompasses skarn, vein/stockwork/breccia (VSB), porphyry, and disseminated/greisen W deposit types (British Geological Survey, 2011). In the magmatic-hydrothermal systems, skarns and VSBs are the most economically significant. Major VSB deposits include Panasqueira (Portugal) and Xihuashan (China). Most VSB deposits form in and/or near granitoid intrusions and vary from high-grade discreet veins (lodes) to lower-grade vein stockworks or breccias. Porphyry W deposits are similar but are typically associated with shallower, subvolcanic intrusions; a major example is Logtung in Canada. Disseminated/greisen systems can form distinct deposits (e.g., Shizhuyuan, China), but this style of mineralized rock can be found in the other deposit types. The overlap of these deposit types in the mineral system makes compilation of robust grade and tonnage models for each type difficult because an individual mine or deposit may include distinct orebody morphologies from different parts of the mineral system that are mined using different methods and cutoff grades. Consequently, this study focuses only on W skarn as it is the most economically significant, forms a discreet part of the mineral system, and is the deposit type most amenable to assessing using the available datasets in the study area.

Although skarns can form through reaction of many types of fluids, they typically form through contact metamorphism and metasomatism of sedimentary or metamorphic rocks along the contact of an igneous body, most commonly forming in carbonate-bearing units. Skarns are typically classified based upon their dominant calc-silicate mineralogy, such that magnesian skarns consist of Mg silicates formed in dolomite and calcic skarns consist of Fe—Ca silicates that replace limestone. However, from a resource standpoint, skarn deposits can also be classified by their economic metal content (Meinert, 1992). Major skarn deposit types include iron (Fe), gold (Au), copper (Cu), zinc (Zn), molybdenum (Mo), tin (Sn), and tungsten (W). Besides differences in metals, these skarn types may show differences in depth of formation, type of causative pluton, and host rock. For further detailed information, readers are referred to major reviews including Einaudi et al. (1981), Newberry and Einaudi (1981), Newberry and Swanson (1986), Kwak (1987), Meinert (1992), and Meinert et al. (2005).

Generally, W skarns are associated with calc-alkaline, I-type stocks related to continental margin orogenic belts (Einaudi et al., 1981), but they can also be associated with S-type intrusions. Crustal contamination is a characteristic feature of the causative pluton, but no correlation between deposit size and degree of crustal contamination has been noted (Anderson, 1983; Sawkins, 1984). Prolonged magmatic activity occurs within orogenic belts, but specific periods are likely to form fertile skarns versus barren skarns. For example, late- to post-orogenic magmatism is associated with fertile skarn formation in the Variscan orogenic belt whereas barren skarns are associated with peak regional magmatism (Burisch et al., 2019). Late- to post-orogenic magmatic events are of importance for W skarn formation in Canada and in the Yukon-Tanana Upland study area. Scheelite-bearing W skarns can be associated with a variety of granitoid compositions ranging from diorite to granite but are commonly associated with felsic granodiorite and granite intrusions. The intrusions themselves are generally coarse grained and likely to contain K-feldspar megacrysts that are related to the vapor undersaturated conditions of the magma (Swanson, 1977). Even though the granitoids generally have low W and water contents, they are the source of W in the skarns (Newberry and Swanson, 1986). Significant fractional crystallization is thought to concentrate W into the remaining magma before being partitioned into a saline fluid exsolved late from the evolved magma; Newberry and Swanson (1986) suggest that perhaps 99% crystallization would be typical for the igneous rocks associated with scheelite skarns and the W content of the residual magma could rise to 300 ppm.

Tungsten skarns are mostly calcic skarns as indicated by the dominance of andraditic garnet or hedenbergitic pyroxene. As noted in deposits from the Canadian Cordillera, this is because dolostones inhibit the development of W skarns, and hence, magnesian W skarns are rare (Ray, 2013). Instead, they commonly form in Ca-rich argillaceous carbonate rocks and intercalated beds of carbonate-pelite or carbonate-volcanic sequences within high temperature metamorphic aureoles surrounding batholiths (Einaudi et al., 1981; Meinert, 1992). Permeability of the host sequence further affects potential formation of an economic skarn through the availability of carbonate for reaction. This is especially true when impermeable aquitard units, such as hornfels, underlie and overlie the reactive unit and force fluids to flow laterally through a calcareous layer. Permeability of the host rock may be reduced due to an elevated metamorphic grade which would inhibit skarn formation. Deformation and structural dismemberment may also decrease the lateral continuity–and thereby maximum potential volume– of carbonate units.

The textures of the causative pluton (K-feldspar megacrysts, absence of porphyry textures) indicate that W skarns form in deeper environments than other skarns, such as Cu or Zn + Pb skarns. Crystallization pressures of >1 kbar, and most with >1.3 kbar, are estimated (Newberry and Swanson, 1986). Meinert et al. (2005) concluded that depth of formation fundamentally controls the size, geometry, and style of alteration associated with skarn deposits. Intrusive contacts at the depths where W skarns form are prone to be subparallel to bedding as intrusion occurs along bedding planes or as the sedimentary rocks deform toward alignment with the intrusive contact. In deeper environments where W skarns form, an exoskarn is typically restricted to a narrow but vertically extensive zone that forms a shell tens to hundreds of meters away from the causative pluton (Meinert, 1992; Dawson, 1996). However, this generalization has numerous exceptions such as the flat-lying ore bodies of Mactung (Dick and Hodgson, 1982) and Agylki, eastern Siberia (Soloviev et al., 2020). Ultimately, ore geometry is dependent upon the morphology of the reactive host rock.

Unlike many other types of skarn deposits, W skarns can have either reduced (e.g., pyrrhotite and ferrous iron-rich calc-silicates) or more

oxidizing (pyrite, andradite garnet, and epidote) mineral assemblages. These distinct redox assemblages are partially dependent on depth of formation and host rock carbon content (Newberry, 1982). Commonly, reduced W skarns tend to be larger than their oxidized counterparts (Meinert, 1992). Considering that the W skarns found in the Northwest and Yukon Territories are reduced (Dick, 1980), any significant undiscovered W skarns in eastern Alaska would likely also be reduced in nature due to similarities in potential host sequences. The likely reduced nature of any undiscovered W skarns is further expected due to the presence of reduced W skarns near Fairbanks (e.g., Stepovich mine) and the multitude of reduced intrusion-related gold and orogenic gold deposits located within these terranes. Carbonaceous wall rocks will tend to produce abundant pyrrhotite and calc-silicate minerals such as hedenbergite clinopyroxene and almandine garnet as part of the assemblage of these reduced scheelite-bearing skarns (Newberry and Swanson, 1986). Similar depths of formation, collisional/subduction tectonic settings, and Au—W geochemical associations mean that W skarns are likely to be found in orogenic Au and reduced intrusion-related Au provinces (Thompson et al., 1999; Soloviev et al., 2020) such as in the Yukon-Tanana Upland study area. Tungsten skarns have a range of geochemical associations that include Sn, Mo, Cu, Be, Bi, Ag, Zn, As, Fe, and Mn (Cox, 1986; British Geological Survey, 2011).

2.2. Grade and tonnage model

Grade and tonnage models provide analogues for the possible size distribution of undiscovered resources of region using the three-part form of assessment. The estimation of undiscovered resources requires an appropriate grade and tonnage model, preferably using a model that incorporates the most recent and best quality data available. The need to account for factors such as updates to mineral inventory reporting standards, expanded mineral inventories due to additional exploration at known deposits (Fig. 2A), and the inclusion of important Chinese deposits (which until recently were unknown or poorly described), prompted the development of an updated W skarn grade and tonnage model (Green et al., 2020) that contains 41 deposits worldwide, including 6 deposits in the Yukon and Northwest Territories of Canada (Fig. 2).

To determine if a more specific regional grade and tonnage model may be appropriate for application to a given regional study area, testing for the presence of statistically distinct sub-populations in the global grade and tonnage model is necessary. The absence of Alaskan deposits within the global grade and tonnage model resulted in the use of Canadian deposits in the Yukon and Northwest Territories as a proxy for potential Alaskan deposits because they share a similar geological setting. We conducted a Student's *t*-test statistical analysis to compare the means of the populations of log-transformed tonnages and grades of the 6 Canadian deposits to the other 55 deposits in the model (Fig. 2B, C) to determine if the Canadian deposits' grades and tonnages are statistically different from other global deposits. Although the tonnages of the Canadian deposits are highly variable, the mean is not distinct from the set of global deposits. The presence of a statistically distinct set of values for grade between the regional Canadian deposits and the global model as a whole is not likely to have a significant impact on the estimation of undiscovered economic resource potential in the Yukon-Tanana study area because the mineral inventory of a deposit is primarily controlled by its tonnage, whereas grade values more strongly influence the return rates of producers (Singer, 1995). The lack of a statistically distinct mean tonnage value between the Canadian deposits and the global model is therefore a strong indicator that the global model may be appropriately applied in the Alaska Yukon-Tanana study area and that the need for a specific regional model does not exist here.

3. Geologic background

3.1. Regional geology

The Yukon-Tanana Upland (YTU) is a complex region made up of late Proterozoic(?) and Paleozoic metamorphic rocks and younger intrusive rocks, bound to the south by the Denali fault and to the north by the Tintina fault (Figs. 3, 4). The YTU consists of two major groups of rock assemblages, the allochthonous arc and basinal assemblage of the Yukon-Tanana terrane (YTT) and the continental marginal assemblages of parautochthonous North America (Fig. 4). The YTT was rifted from the North American continent in the Late Devonian and subsequently multiply intruded by magmas; the best-exposed igneous rocks are Triassic and Early Jurassic (Piercey et al., 2006). The YTT was re-accreted to North America over an extended period, from the Permian to Jurassic (Mortensen, 1992; Hansen and Dusel-Bacon, 1998; Dusel-Bacon et al., 2002; Beranek and Mortensen, 2011). The originally inboard parautochthonous North America was impacted by magmatism during Devonian rifting, followed by quiescence until the initial re-accretion of the YTT. During the Jurassic, the YTT was thrust over the landward parautochthonous rocks (Hansen and Dusel-Bacon, 1998; Dusel-Bacon et al., 2002, 2015). The thrusting caused regional deformation and metamorphism (Dusel-Bacon et al., 1995; Berman et al., 2007). Exhumation of rocks from paleodepths of up to 20 km occurred regionally during the Cretaceous (Hansen and Dusel-Bacon, 1998; Dusel-Bacon et al., 2002). The Fortymile assemblage and associated rocks, along with panels of the Ladue River unit are mappable vestiges of the YTT (Fig. 4).

Mapping of the Yukon-Tanana Upland was mostly completed at 1:250,000 or 1:63,360 scales, with general classification of different Paleozoic units compiled by Wilson et al. (2015). Most geologic units in the study area are dominated by greenschist to amphibolite facies siliciclastic and/or volcaniclastic rocks. Subordinate limestone/marble beds have been recognized but were not systematically mapped across the study area in most initial mapping efforts (e.g., Weber et al., 1978; Foster, 1976, 1992; Dusel-Bacon et al., 1993), hence are not distinguished in the Wilson et al. (2015) compilation.

We combined compositionally similar geologic rock units of Wilson et al. (2015) from individual geologic terranes to create a simplified geologic map that approximates the map of Dusel-Bacon et al. (2017). Units mapped as predominantly quartzite and quartz-mica schist (e.g., Birch Creek schist and informally named Cleary sequence; PzPygs, −qs, −qm units of Wilson et al. (2015)) are collectively colored light blue in Fig. 4. Keevy Peak Formation and similar units (Pzkp; dominantly phyllite, meta-argillite, quartzite, and chert) are colored gray, and Totatlanika Schist (schists, augen gneiss, metavolcanic rocks, and greenstone) are colored green in Fig. 4. Carbonate units are not described in gneiss and orthogneiss-rich units (MDAG and Pzymi) of Wilson et al. (2015) (dark blue, Fig. 4).

The main metamorphic rock units mapped in the allochthonous YTT panels, Klondike schist (Pks; pale green) and Fortymile assemblage (orange; Fig. 4), also contain carbonate (marble) (Wilson et al., 2015, and references therein). Klippe and blocks of obducted oceanic crust and related metasedimentary rocks, including the Seventymile terrane and Chatinika assemblage (near Fairbanks), are scattered across the region with most coherent blocks of Seventymile terrane in the northeast of the study area.

Several periods of arc-related magmatism have impacted the YTU. Late Triassic and Early Jurassic intrusions are confined to the YTT in the Fortymile River assemblage and related arc and basinal assemblages (purples, Fig. 4). Triassic magmatism is restricted to the Taylor Mountain batholith and nearby stocks of diorite and monzodiorite composition ("Tr," Fig. 4; Dusel-Bacon et al., 2015, 2017). The Jurassic suite of intrusions is somewhat more spatially extensive and has compositions that range from monzonite to granite ("eJ", Fig. 4; Dusel-Bacon et al., 2015). These relatively old intrusions show variable degrees of foliation

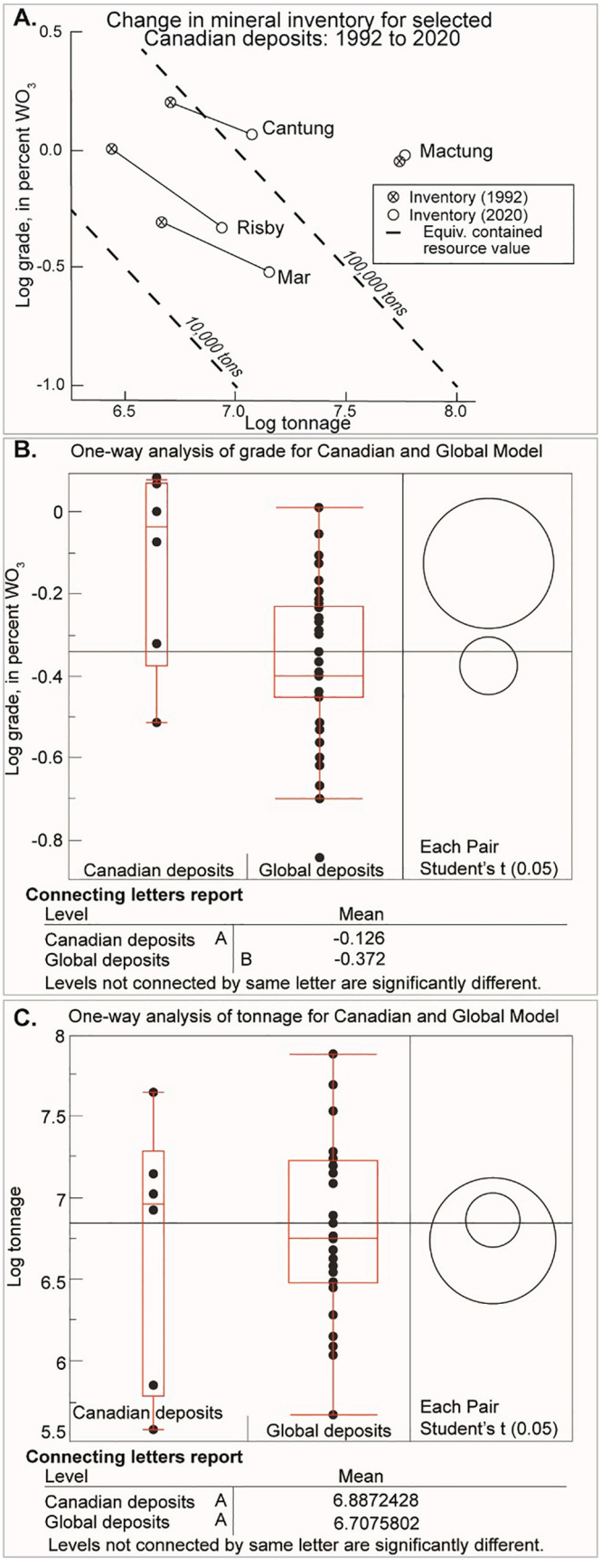

(caption on next column)

Fig. 2. Aspects of grade and tonnage modeling to the YTU assessment. A) Change in contained W values from the Menzie et al. (1992) grade and tonnage model (g-t model) to Green et al. (2020) model for selected Canadian W skarn deposits. In all four deposits, apparent contained WO_3 has increased in more recent reporting despite average grade decreasing (except Mactung). Acknowledgements to Graham Lederer (USGS) for producing this fig. B) Distributions and Student's *t*-tests for log-transformed average WO_3 grades for six Canadian W skarn deposits compared to all other W skarn deposits included in the global g-t model of Green et al. (2020). Note the contrasting grade distributions in box plots and that the "Each Pair" student's t ellipses do not overlap and the connecting letters report indicate two populations (A and B), indicating that Canadian deposits' grades as a group are statistically distinct (and higher) than the remainder of deposits included in the global g-t model of Green et al. (2020). C) Distributions of log-transformed tonnage values for the same deposit groupings as (B). Log tonnage values are similar and are not statistically different between the Canadian and other deposits included in the global g-t model, as demonstrated by the co-located "Each Pair" ellipses and the "A" classification for both populations in the connecting letters report. (For interpretation of the references to colour in this figure legend, the reader is referred to the web version of this article.)

imparted during subsequent Jurassic overthrusting events.

Middle Cretaceous intrusions, which generally postdate thrusting and subsequent regional exhumation, are widespread in the parautochthonous North American assemblages to the northwest, west, and south of the YTT. These intrusions (red – "mKg," Fig. 4) obscure the exact location of faults related to overthrusting by the YTT in the Jurassic. Spatially extensive to the east of the Shaw Creek fault, they occur only as small isolated bodies to the northwest, including northeast of Fairbanks. Compositions span from granodiorite to granite, with calc-alkaline and weakly peraluminous character (Hart et al., 2004).

Late Cretaceous to early Tertiary intrusions (dark pink – "lKg," Fig. 4) are more broadly distributed across the study area, but their individual exposures at the surface are smaller than the middle Cretaceous intrusions. In the Circle area, the intrusions range mostly from granodiorite to syenogranite and are ilmenite dominated, with I-type characteristics, similar to middle Cretaceous plutons in the Fairbanks area (Newberry et al., 1990). Farther to the east, studied plutons are predominantly quartz monzonite, granodiorite, and granite, with local syenite bodies; these plutons are metaluminous to weakly peraluminous chemistry, likely derived from mildly oxidized, mantle-sourced magmas (Dusel-Bacon et al., 2015; Kreiner et al., 2019). Late Cretaceous and Tertiary age volcanic rocks are preserved almost exclusively to the east of the Mount Harper lineament (Fig. 4).

The Tintina fault separates the YTU allochthonous and parautochthonous rocks from North American cratonic rocks to the northnortheast, whereas the Denali fault marks the boundary between the YTU rocks with more recently accreted Wrangellia terrane and related rocks to the south-southwest (Nelson and Colpron, 2007). Timing of initial movement along the faults has been interpreted as Eocene or younger for the Tintina fault (Gabrielse et al., 2006). Initial movement on the Denali and subsidiary faults likely occurred by the middle Cretaceous (e.g., Richter et al., 1975; Miller et al., 2002; Manuszak et al., 2007; Trop et al., 2020). Based on field studies, both faults record dextral displacements ranging from 340 to 450 km.

A series of northeast-trending lineaments and faults with sinistral and oblique-extensional dip-slip displacement cut the study area (e.g., Page et al., 1995; Dusel-Bacon and Murphy, 2001; O'Neill et al., 2010; Sanchez et al., 2014). These faults are interpreted to be a consequence of the dextral shear along the Tintina and Denali faults. O'Neill et al. (2010) suggested that the northeast-trending Black Mountain tectonic zone was active since the middle Cretaceous, based on geophysical breaks and co-location with middle Cretaceous plutons, which could indicate middle Cretaceous timing for initial movement of both the Tintina and Denali faults.

The NE-trending faults created displaced structural blocks, as noted by Newberry et al. (1998). Mesozoic intrusions are extensively exposed,

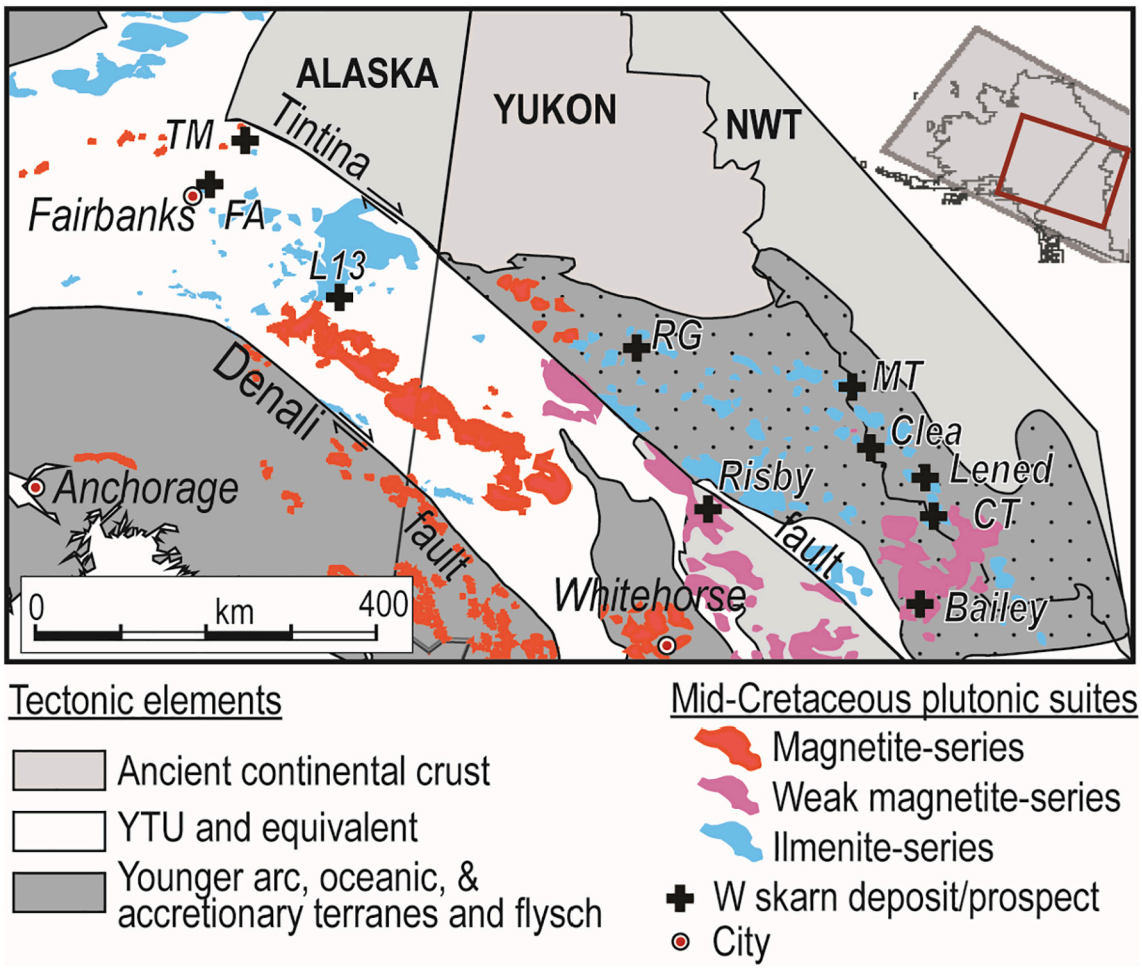

Fig. 3. Simplified map of parts of eastern Alaska, and Yukon and Northwest Territories (NWT), Canada, showing major tectonic elements, distributions of middle Cretaceous magnetite-, weak magnetite-, and ilmenite-series intrusions, and locations of major W skarn deposits/prospects. Note the association of W skarn with reduced, ilmenite series intrusions in YTU and equivalent rocks. Modified after Hart et al. (2004). Abbreviations for deposits/prospects as follows: in Alaska—FA – Fairbanks area, TM – Table Mountain, L13 – Lucky 13; in Canada—RG – Mar/Ray Gulch, MT – Mactung, CT – Cantung.

as well as preserved YTT rocks and Cretaceous and younger volcanic rocks to the east of the Mt. Harper lineament, features that are lacking to the west (Fig. 4).

3.2. W deposits in the study area

Several studies have focused on W skarns and/or their associated intrusions in parts of the Yukon-Tanana Upland (Newberry and Swanson, 1986; Newberry et al., 1998; Hart et al., 2004). The best-known examples of W skarn in the study area are in the Fairbanks area, and the Table Mountain and Lucky 13 prospects (Fig. 4, Table 1).

The Fairbanks district contains 12 known W skarn occurrences and 9 placer prospects with reported W (Figs. 3, 4; https://mrdata.usgs.gov/ardf/). The primary skarn occurrences are northeast of Fairbanks on Pedro Dome and Gilmore Dome (Fig. 4). Historical mines on Gilmore Dome have the only recorded W production in the YTU. The skarns occur within Devonian calcareous units of the informally named Cleary sequence (Aleinikoff and Nokleberg, 1989) intruded by the Cretaceous (90 Ma; Allegro, 1987) granite and granodiorite of Gilmore and Pedro Domes. Thin 0.3- to 2 m-thick marble beds are interbedded with schist and quartzite of the Cleary sequence (Byers Jr., 1957; Allegro, 1987). The skarns are typically zoned from garnet dominated near the intrusive-carbonate contact outward to pyroxene-garnet to wollastonite-idocrase assemblages; the greatest W (scheelite) and Au enrichment is in the pyroxene-rich zone (Allegro, 1987; Newberry et al., 1998). The grade and nature of the mineralized zones vary from occurrence to occurrence. Mineralized zones are irregularly distributed along strike and can be localized along structural surfaces or in crosscut stratigraphy and are commonly associated with quartz veining (Allegro, 1987). Hall (1985) noted four distinct deformational phases in the Fairbanks area, lending to the discontinuous nature of the carbonate units in the Cleary sequence, and dislocation structures related to the emplacement of the Cretaceous plutons host the W skarns. Historical production from the Stepovich mine, Gilmore Dome, was 4000 units (40 t) of WO_3 (Byers Jr., 1957); an estimated remaining resource of 20 kt at 0.5–3.6%WO_3 was reported by Nokleberg et al. (1987). Rocks from the prospects in the Fairbanks area commonly contain elevated concentrations of Cu, Pb, Zn, Ag, Mo, Sn, As, and F as well as W (Allegro, 1987, Appendix IV).

Several Au-bearing W skarns have been identified at Table Mountain, 160 km northeast of Fairbanks (Fig. 4). These mostly small (60 × 75 m) W—Au skarns share similar alteration, mineralization assemblages, and host rocks as the W skarn in the Fairbanks area (Allegro, 1987; Newberry et al., 1987). They are interpreted to be genetically related to the nearby middle Cretaceous Mt. Pinnell pluton (Newberry et al., 1987). Calcareous and calc-silicate rock samples from reconnaissance sampling in the Table Mountain area contained up to 500 ppm W (Foster et al., 1983; Menzie et al., 1983), and stream sediment heavy mineral concentrate mineralogy and chemistry indicate a broad distribution of scheelite and W (Tripp et al., 1986, plates 1 and 2). Eleven composite samples from trenches in the skarn occurrence have average reported values of

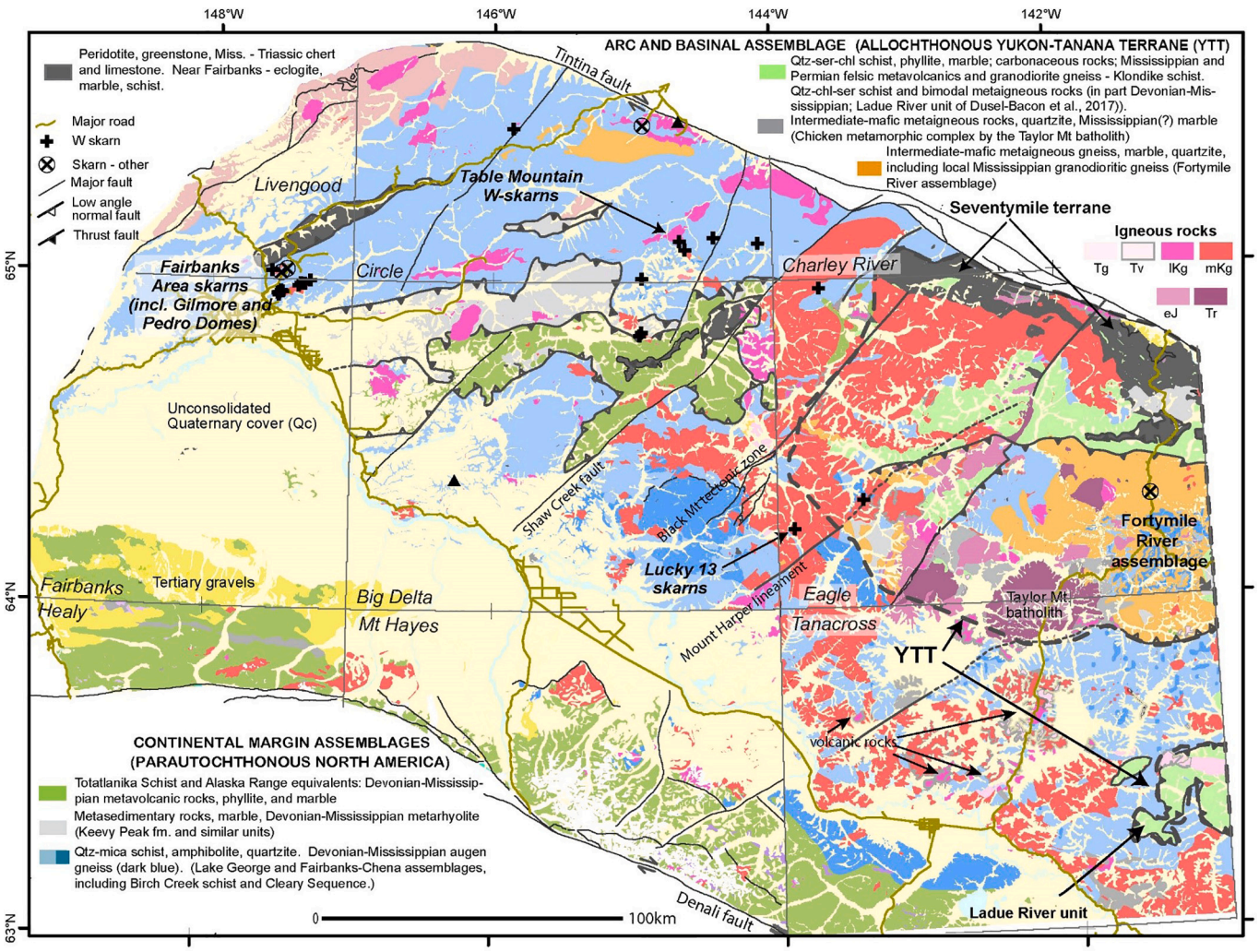

Fig. 4. Generalized geology of the Yukon-Tanana Upland with locations of known W and other skarn occurrences/deposits. Igneous rocks include Triassic (Tr), Early Jurassic (eJ), middle Cretaceous (mKg), latest Cretaceous to early Tertiary (lKg), and Tertiary (Tg). Volcanic units are colored by age but with outline in light gray (e.g., Tv). Quadrangle boundaries are shown for reference. Modified from Wilson et al. (2015) and Dusel-Bacon et al. (2017).

1041 ppm W, 91 ppm Cu, 157 ppm Sn, 234 ppm Zn, and 96 ppb Au (Newberry et al., 1987). Unaltered-unmineralized Tertiary rhyolite dikes cut the skarn (Newberry et al., 1987). Tertiary and Cretaceous plutons to the west, including Lime Peak (57 Ma), Quartz Creek (66 Ma), Mt. Prindle (60 Ma), and Pinnell Trail (90 Ma) (Newberry et al., 1987) contain occurrences with combinations of elevated Sn, W, Au, and/or Sb. Table Mountain is northwest of the regional left lateral Swamp Saddle fault (Newberry et al., 1987). Gold occurrences in the area are noted to be associated with structure; however, there is no description of structure in relation to the W-bearing skarns (Menzie et al., 1983; Menzie et al., 1987).

The Lucky 13 skarns are located approximately 200 km southeast of Fairbanks (Figs. 3, 4). The skarns occur in a roof pendant of calc-silicate- and siliceous-marble-bearing gneisses and amphibolites along the margin of a 94.2 ± 0.3 Ma quartz monzonite (Huskey, 1981; Newberry et al., 1998). Though the calc-silicate rock units are volumetrically minor, most contain at least minor scheelite and chalcopyrite in banded to massive skarns consisting of scheelite, pyrite, pyrrhotite, chalcopyrite, and minor molybdenite as well as garnet, pyroxene, epidote, and quartz (Union Carbide Corp., 1979). Amphibolite locally contains scheelite associated with pyrite, pyrrhotite, chalcopyrite, galena, and sphalerite. Many of the skarns around Mt. Good are small (>3 m thick), irregular, and discontinuous. The largest body is ~75x5x9 m in size and contains as much as 4.16% WO_3; three pods within this body average 1.5% WO_3. An historical aggregated resource estimate was ca. 20 kt of 1.5% WO_3 (Union Carbide Corp., 1979). Based on drilling, skarn may be steeply dipping (~60 degrees; Huskey, 1981), with additional skarn or porphyry potential below the depth of drilling (Hughes and Siems, 1980).

In contrast to the limited number and size of known and exploited W skarns in eastern Alaska, significant W skarn deposits occur in the Yukon and westernmost Northwest Territories, Canada (Fig. 3; Table 1). Some of these deposits occur in rocks that generally correlate to those of the Fairbanks area–with similar intrusion chemistry, structure, and mineralization styles–suggesting that the rocks in the Fairbanks area and the Yukon were adjacent to one another before the Cretaceous to early Tertiary offset of the Tintina fault (Engebretson et al., 1985; Hart et al., 2004; Mair et al., 2006). Six deposits, including Cantung, Mactung, Lened, Mar/Ray Gulch (RG), Bailey, and Risby deposits, are sufficiently delineated to be included in the Green et al. (2020) grade and tonnage model for W Skarns (Table 1). Cantung, Mactung, and Lened (along with the Clea prospect) (Fig. 3) lie along the transition between the Selwyn Basin clastic rocks and carbonates of the Mackenzie Platform, the latter of which contains appreciable limestone, a feature absent from the Alaska study area. Three of the deposits occur a little farther to the west in Selwyn Basin (Mar/Ray Gulch (RG in Fig. 3) and Bailey) and the Cassiar Platform (Risby). The skarns are all associated with ~middle Cretaceous ilmenite-series to weak magnetite-series granite to

Table 1
Example W skarn deposits of the assessment area and northwest Canada.

Deposit		Pluton Age	Stratigraphic unit	Skarn assemblage	Resource	Status
Alaska Examples						
1	Fairbanks area	90 Ma	Cleary sequence	garnet-dominated to pyroxene-garnet to wollastonite-idocrase assemblages	20,000 t at 0.5–3.6% WO_3	Past Producer
2	Table Mountain	90 Ma	Cleary sequence equiv.	garnet, clinopyroxene, chlorite, and amphibole skarn minerals; rare pyroxene-pyrrhotite rich skarn	None reported	Undeveloped
3	Lucky 13	94.2 Ma	Paleozoic parautochthonous strata	Scheelite, pyrite, pyrrhotite, chalcopyrite, and minor molybdenite, garnet, pyroxene, epidote, and quartz	~18,000 t @ 1.5% WO_3	Undeveloped
Canadian Examples						
4	Mactung	97.5 Ma (*Re*—Os) 92.1 Ma (U—Pb)	Cambrian to Ordovician limestone of the Selwyn Basin and Mackenzie Platform	garnet-pyroxene and pyroxene-pyrrhotite and scheelite mostly associated with pyrrhotite	44,900,000 t @0.85% WO_3*	Feasibility
5	Cantung	95 Ma	Early Cambrian limestone of the Selwyn Basin and Mackenzie Platform	pyrrhotite or calc-silicate skarn with pyroxene, diopside, garnet, actinolite, biotite, scheelite, +/− chalcopyrite, sphalerite	10,797,000 t @ 1.2% WO_3*	Past Producer/ Inactive
6	Lened	~93 Ma	lower Paleozoic carbonate sequence of the Selwyn Basin and Mackenzie Platform	scheelite in biotite-pyrrhotite facies; minor scheelite in garnet-pyroxene facies	750,000 t @ ~1.17% WO_3*	Undeveloped
7	Clea	~93 Ma	Cambrian to Ordovician limestone of the Selwyn Basin and Mackenzie Platform	scheelite in sulfide-rich or calc-silicate skarn, with zones of pyrite, pyrrhotite, chalcopyrite, and minor sphalerite and bornite.	0.46% WO_3 over 0.7 m and 0.19% WO_3 over 2.6 m	Undeveloped
8	Mar/Ray Gulch (RG)	95 Ma	Neoproterozoic to Early Cambrian metasediments of the Selwyn Basin	clinopyroxene, plagioclase, quartz, grossular garnet, scheelite, calcite +/− amphibole	14,000,000 t @ ~0.31% WO_3*	Undeveloped
9	Risby	103 Ma	Neoproterozoic to Cambrian carbonates of the Cassiar Platform	scheelite in garnet-rich diopside skarn with pyrrhotite, actinolite, and minor pyrite, chalcopyrite +/− molybdenite	8,537,000 t @ 0.48% WO_3*	Undeveloped
10	Bailey	middle Cretaceous	Devonian-Mississippian metasediments of the Selwyn Basin	proximal pyroxene-pyrrhotite-scheelite-chalcopyrite; distal garnet-pyroxene+/−magnetite	405,000 t @ ~1% WO_3*	Undeveloped

References: 1) Allegro, 1987; Nokleberg et al., 1987. 2) Newberry et al., 1987. 3) Union Carbide Corp., 1979; Huskey, 1981; Newberry et al., 1998. 4) Dick and Hodgson, 1982; Anderson and Baker, 1986; Selby et al., 2002; LaCroix and Cook, 2007. 5) Mathieson and Clark, 1984; Bowman et al., 1985; Sinclair, 1986; Hart et al., 2004; Fitzpatrick and Bakker, 2011; Rasmussen et al., 2011; Delaney and Bakker, 2014. 6) Dick and Hodgson, 1982; Glover and Burson, 1986; Nokleberg et al., 2005. 7) Thompson, 1978; Dick, 1980; Godwin et al., 1980; Dick and Hodgson, 1982; Sinclair, 1986; http://data.geology.gov.yk.ca/Occurrence/13385. 8) Lennan, 1986; Brown et al., 2002. 9) Berdahl, 2004; Nokleberg et al., 2005; Desautels et al., 2007. 10) Way, 1974; Dawson and Dick, 1978; Deklerk, 2003. *Green et al., 2020

granodiorite plutons (Godwin et al., 1980; Mathieson and Clark, 1984; Anderson and Baker, 1986; Glover and Burson, 1986; Lennan, 1986; Deklerk, 2003; Hart et al., 2004; LaCroix and Cook, 2007; Delaney and Bakker, 2014). Although the assessment area lacks the thick carbonate-bearing units like those of the Mackenzie Platform, the presence of similar intrusive suites as along the trend in Canada strongly suggests additional potential for this deposit type in the YTU.

4. Materials and methods

4.1. Overview

Assessing undiscovered resource potential is strongly dependent on the quality of data available. Due to heterogeneity of data quality and density in the YTU, we utilize both qualitative and quantitative methods. For the entire study area, we qualitatively assessed W skarn potential using the mineral potential mapping methods of Jones III et al. (2015) and Karl et al. (2016). Additionally, the USGS three-part form of assessment coupled with economic filters is used to quantitatively assess the western YTU where data density and geologic constraints are most significant.

The workflow for the USGS three-part form of assessment encompasses the following phases. The first phase is delineation of lithologies that allow for the deposit type of interest using a defined mineral deposit model (Fig. 5A). Regional geological and geochemical data are compiled and evaluated (Fig. 5B, C). Mineral system and deposit models are used to determine mappable criteria that can be used to select favorable rock types from the input map datasets to outline permissive tracts for a particular deposit type (Fig. 5D). Next, using a global grade and tonnage model for the deposit type and information about past and current production and exploration in the assessment area, experts estimate the number of undiscovered deposits that may be present in the tract at the 90th, 50th, and 10th percentiles of probability (Fig. 5E, F). Monte Carlo simulation is used to combine the tonnage, grade, and undiscovered deposit distributions to give a probabilistic estimate for the in-place amount of undiscovered WO_3 (Fig. 5G; MapMark4; Ellefsen, 2017a, 2017b). In addition, a range of total and economically recoverable contained resources that may be present in the undiscovered deposits is modeled using the Resource Assessment Economic Filter (RAEF; Shapiro and Robinson, 2019). The following sections describe the datasets used to define the permissive tracts for W skarn deposits and the procedures for the qualitative assessment of the entire study area and for the quantitative assessment of the western YTU tract.

4.2. Input data

4.2.1. Geologic maps

Geologic maps are the primary dataset used to delineate permissive tracts (Fig. 5B). In Alaska, most published maps are 1:250,000 reconnaissance scale; few are larger scale and more detailed. These maps were compiled and correlated in the digital Geologic Map of Alaska and database (GMA; doi:https://doi.org/10.3133/sim3340; Wilson et al., 2015). The digital GMA database comprises a vector feature class (the map) and eight associated data tables of different types of geologic information. The geologic data directly attributed in the map polygon features are limited, and the database is structured such that queries for specific rock types or mapped units are made in the related tables and "pushed" to the map feature class through a related field called NSACLASS.

The GMA database also includes compiled geochronological data from rock samples across the state. While these point data were not used in the permissive tract delineation process, they were plotted and

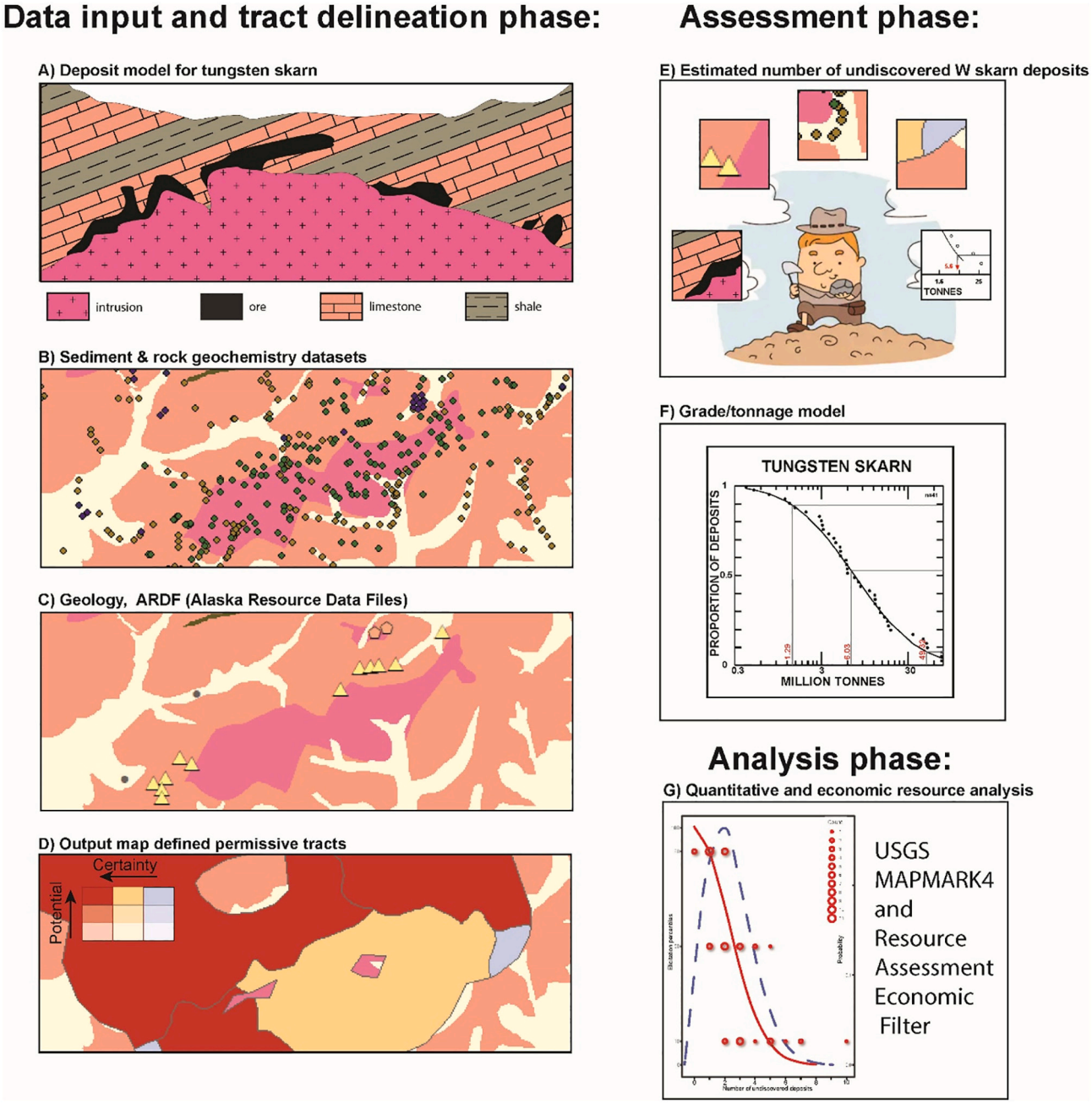

Fig. 5. Workflow of the three-part form of assessment coupled with quantitative and economic resource analysis. Data input and tract delineations phase: A) The deposit model is defined - see Section 2.1. B) and C) datasets are compiled and analyzed. D) An output map of permissive tracts is created with permissive tracts scored by potential and certainty, the qualitative result of the assessment. Assessment phase: E) Undiscovered deposits estimate: With a grade and tonnage model for W skarns defined, the research group reviews the data and scored tracts to estimate the number of unknown deposits that may exist in the tract at the 90th, 50th, and 10th probability percentile (https://www.canstockphoto.com/geologist-6162638.html). F) Grade/Tonnage model defines the endowment of known global deposits (Green et al., 2020). Analysis phase: G) Quantitative and economic resource analysis using the MAP MARK4 simulation combines tonnage, grade, and the number of undiscovered deposits to estimate the potential amount of contained metal, and RAEF runs engineering mine cost analyses. It estimates potentially recoverable resource based on deposit type, grade, tonnage, depth, and regional production cost.
(For interpretation of the references to colour in this figure legend, the reader is referred to the web version of this article.)

analyzed to help identify spatiotemporal trends in plutonism and mineralization that might indicate underlying regional differences in W skarn potential.

4.2.2. Mineral site data

The Alaska Resource Data File (ARDF; https://ardf.wr.usgs.gov/index.php), which summarizes all known mineral sites in Alaska, was used as the source for locating and describing W-bearing mines, prospects, and occurrences (Fig. 5B). Within the nine assessed quadrangles, a total of 163 sites that contained W as a commodity were individually evaluated for deposit type classification; missing, outdated, or incorrect deposit type information was updated. Of the 163 sites, W was considered a main commodity in ~40 sites coded as skarn, porphyry Mo, pegmatite, orogenic gold, or placer.

Mineral sites for which W is a main commodity were ranked for their significance based on the criteria shown in Table 2. The highest possible rank is 10, which would be assigned to W skarn deposits with a National Instrument (NI) 43–101- or Joint Ore Reserves Committee (JORC)-

compliant tungsten resource definition. The lowest rank is 1, which includes lode or placer prospects or occurrences that may be related to a W skarn mineral deposit. No sites in the study have a defined W resource (rank 10), but four past producing W skarns located in the vicinity of the Fort Knox gold mine were given the next highest ranking of 5. For assessment purposes, the locations of lode W skarn deposits are considered the most important; placer deposits were considered as vectors toward potential deposits.

4.2.3. Geochemical and mineralogical data

The geochemical datasets used in this assessment (Fig. 5C) are derived from the USGS Alaska Geochemical Database 3.0 (AGDB3; Granitto et al., 2019), which contains data for samples of geological materials collected across Alaska. The AGDB3 is the most recent compilation of new and legacy geochemical analyses of rock, stream sediment (hereafter called, "sediment samples"), soil, mineral, and heavy-mineral concentrate (HMC) samples in the state. Within the YTU study area, the AGDB3 includes geochemical analyses of ca. 19,800 rock samples, 20,000 sediment samples, and 7500 HMC samples collected between the 1960s and 2017 and prepared according to various USGS standard methods (Granitto et al., 2019, and references therein). The geochemical and mineralogical data in AGDB3 were analyzed and synthesized into a geodatabase for this assessment. Soil and mineral geochemical samples were excluded due to extremely sparse coverage in the study area.

Many samples in the AGDB3 datasets were analyzed by more than one method; consequently, these samples have multiple concentration determinations for some elements. To minimize the complexity inherent in multiple determinations for individual elements, a single 'best value' concentration was identified for each element in each sample. The best value for an element was determined by ranking each combination of digestion and analytical method based on its suitability for that element. As an example, for a sample with multiple ICP-MS analyses for W–one a partial digestion (e.g., aqua regia) and one a total digestion/decomposition (e.g., fusion)– only the determination from the total digestion analysis is used in the concentration field of the table. Granitto et al. (2019) provide a more detailed description of the ranking criteria for the analytical methods and how they were used to determine best values. Most of the best value determinations for W and Sn in the study area were made via either six-step semi-quantitative direct arc-emission spectrography (ES_SQ), neutron activation (NA; mainly used in National Uranium Resource Evaluation samples), or energy-dispersive X-ray fluorescence spectrometry (EDX). These methods generally have high detection limits (DLs) for W and Sn (2–200 ppm). <30% were analyzed via more modern methods that have lower detection limits (<1 ppm) (e.g., inductively coupled plasma-mass spectrometry [ICP-MS] after Li-borate fusion [MS_Fuse] and ICP-MS after four-acid digest). All of these methods are quantitative except ES_SQ, which is semi-quantitative. Information about the individual analytical and digestion methods and their range of detection limits for each element are documented in Granitto et al. (2019). About 80 stream sediment samples from AGDB3 in the study area were reanalyzed in 2019 via ICP-optical emission spectroscopy (OES) following Na-peroxide fusion (Wang et al., 2021) and included in this assessment. Cox (1986) listed W skarn deposit trace element chemistry to include W, Mo, Zn, Cu, Sn, Bi, As, Fe, and Mn. Due to the variety of analytical methods, inconsistencies in the element suite analyzed, and variability in detection limits between analytical procedures, only Sn and W were used in the assessment. Additionally, Bi, As, Zn, and Cu are more indicative of other deposit types.

In addition to the geochemical samples, the database also contains mineralogical data, including reported occurrences of scheelite and cassiterite, from about 2200 non-magnetic heavy-mineral concentrate samples in the study area. Mineralogy for these samples was determined visually and reported qualitatively as 'present' or 'abundant,' or semi-quantitatively as relative percent abundance.

Table 2
Site ranking criteria used to assess importance of W-bearing localities.

Rank	Deposit Type	Criteria
10	Skarn	Known deposit with reliably identified W resources
5		Past W producer or explored prospect with some resource data
4		Past W producer or prospect with no resource data or data suggest low grade or too small. May have been mined for a different commodity.
3		W skarn occurrence with no resource data available
2	Other W deposit type (porphyry, orogenic, pegmatite, placer)	Prospect or occurrence with W; scheelite mentioned among minerals present
1		Prospect or occurrence with W. Placer could be related to an upstream W skarn site

4.2.4. Geophysics

Publicly available geophysical data for the assessment area include airborne magnetics and surface gravity. Airborne magnetic data are from a NOAA compilation by Miles et al. (2017). Gravity data are from a compilation of Alaska Gravity Data and Historical Reports database (Saltus et al., 2008) and the BGI World Gravity Map (WGM) (Bonvalot et al., 2012). These data types provide petrophysical evidence that may be associated with W deposits.

The Free Air Anomaly (FAA) gravity data show a positive correlation with known W mineralized sites, but these data are also highly correlated with topography. The Complete Bouguer Anomaly (CBA) map shows no anomalies in the study area that correlate with known W skarns after topographic effects are corrected and the CBA is gridded and plotted.

The merged airborne magnetic datasets were processed to enhance magnetic contrasts caused by structures, magnetite-bearing alteration, or igneous bodies. Processed reduced to pole magnetic data delineate structures under cover. In these areas, the geophysics were used to modify geologic contacts when creating the regional geologic map (Wilson et al., 2015, and references therein). Specific to the assessment, mineralized zones <1 km in depth were considered and data were further processed using the analytic signal and local wavenumber (Nabighian, 1972; Phillips, 2002; Pilkington and Keating, 2006) to enhance shallow igneous intrusions. Unfortunately, the mappable intrusions do not consistently correlate with known W skarn occurrences. Due to low resolution it is impossible to separate geophysically anomalous zones of the older W-related igneous bodies from the often-coincident younger intrusive suites using the magnetic data alone. Higher-resolution data are necessary to better incorporate geophysics directly into any future assessments of regional mineral potential.

4.3. Delineation of permissive tracts

W skarn-related mineral systems and W skarn descriptive models were used to identify salient geologic characteristics that could be extracted as mappable criteria from the digital GMA and geochemical databases to create permissive tracts. The key criterion that defines the permissive tract is the intersection of carbonate-bearing sedimentary/metasedimentary rocks with differentiated felsic granitoids. We chose to focus on carbonate-bearing rocks because they are by far the most favorable country rock type for skarns, including known occurrences in the study area. The type of granitoid intrusion for the purposes of this study is deliberately broad. Ideally, other information about the felsic intrusions–their composition, emplacement depth, and exposure level–would allow unfavorable granitoids to be excluded. However, due to poor exposure and coarse-mapping resolution in the study area, the precise spatial extent and composition of granitoid and carbonate rock

types are difficult to determine. For this reason, an inclusive approach, using all mapped granitoid intrusions, was taken to generate permissive tracts in this assessment.

Using GIS software, the permissive tracts were generated by creating a 2 km buffer around the intersections of carbonate-bearing rocks and granitoids. Carbonate-bearing rock packages were selected by using both the nsaunits and nsalith tables in the GMA database. The full list of keywords from both tables is shown in Supplementary Data A. The nsalith table contains hierarchical rock type classifications that range from general classes such as igneous in field LITH1 to more specific names like syenogranite in field LITH5. This table has a one-to-many relationship with the map feature class; therefore, a map feature may have multiple nsalith rock types. The fields LITH2, LITH3, and LITH4 were searched for carbonate rock type keywords such as limestone and marble, but not dolostone; LITH5 was excluded because it is mostly empty. The nsaunits table contains detailed stratigraphic unit descriptions taken from the source maps. The nsaunits table has a one-to-one relationship with the map; each polygon has only one associated stratigraphic unit. The field DESCRIPTION was searched in nsaunits for permutations of carbonate rock types, along with keywords such as skarn and calc-silicate that imply carbonate protoliths.

Granitoids were selected by querying rock type names (see Sup. A keywords) from both LITH3 in nsalith, and SPECIFIC_NAME from igneous samples in the rock geochemistry (rock_BV) table in the AGDB3. Although W skarn systems are typically associated with more evolved granite compositions, information on the mineralogy, geochemistry, and precise rock type are often missing for intrusive complexes mapped at 1:250,000 scale. Therefore, to be inclusive in favorable intrusive rock delineation, all granitoid rock types present in nsalith and rock_BV were selected. The rock_BV point dataset was included to help compensate for such coarse mapping, as many of the intrusions sampled for lithogeochemistry were not mapped. Due to the variation in geochemical analytical methods and the lack of major-element data for many rock samples, rock geochemistry was not used for selecting permissive intrusions. The output selections of carbonate rocks were filtered to remove any rocks younger than Cretaceous. Next, buffers were created around polygons of both selections. Buffering rock contacts accounts for potential variability in the distance between a deposit and the carbonate-intrusive rock contact, for subsurface extensions, and for topological mapping errors. A 2 km buffering distance was chosen because this encompasses the spatial extent of W skarn mineral sites around the Gilmore Dome pluton and is compatible with plausible extent in the deposit model. An initial "prototract" was then generated by intersecting the buffered carbonate and intrusive rock layers using GIS tools. Aggregation and smoothing GIS tools (see Sup. B for parameters) were applied to the prototract to eliminate buffering artifacts and join proximal but isolated tracts that are likely to be continuous.

4.4. Mineral potential mapping methods

An automated Python script (Supplementary Data D) was developed to score for mineral potential using expert-defined scoring parameters and weights applied to the AGDB3 and ARDF datasets to qualitatively assess potential for W skarn mineralization within the permissive tracts across the entire study area. The conceptual workflow and parameters of the automated script are described here and the general approach follows that of Jones III et al. (2015) and Karl et al. (2016), which utilizes watersheds defined in the National Watershed Boundary Dataset (NWBD; U.S. Geological Survey and Dept. of Agriculture, 2013) as the basis of mapping mineral potential. The NWBD defines multiple levels of drainage basins. The most appropriate drainage-basin level for this assessment is level 6, formerly called a subwatershed, which averages 100 km^2 in area. Each level 6 drainage basin is designated by a 12-digit Hydrologic Unit Code (HUC); hereafter, these subwatersheds are referred to as HUCs or stream drainage areas. The choice of HUCs enables mapped potential to be more naturally represented, particularly in the context of stream sediment geochemical samples that primarily drive scoring and are unsuitable for gridding.

Tract HUCs were scored in two parts. First, if the HUC contained one or more W-bearing ARDF mineral sites, it received the ranking value (Table 2) of the highest-ranked ARDF site present multiplied by 2. The multiplication allows the ARDF score to be weighted appropriately with respect to the geochemical scoring. Second, W and Sn concentrations from stream sediment, rock, or HMC geochemical samples were queried, along with relative abundances of scheelite and cassiterite in HMC mineralogical samples. The mixed-method nature of the geochemical datasets makes it difficult to apply conventional statistical methods for determining regional background and anomaly values for W and Sn, particularly because the DL of the most common methods is >10 ppm–nearly 10 times higher than the average crustal abundance of W. For this reason, we chose 20 ppm (2× the DL) as the minimum threshold for an anomaly. The concentrations and relative abundances were binned for scoring, such that a HUC would receive 4 points for having a geochemical sample with 20–50 ppm W (anomaly), 6 for 50–100 ppm (2.5× anomaly), and 10 for >100 ppm (5× anomaly). The median values of W concentration in the study area are comparable for stream sediments (5 ppm) and rocks (3 ppm), so the same thresholds and bin multiples are used. Tin received slightly less weighting as it is associated with, but does not guarantee, W enrichment. The high thresholds were chosen due to the prevalence of ES_SQ, EDX, and NA data, all of which have high DLs, in the study area. For the HMC mineralogical data, qualitative terms such as "Abundant" were binned together with semi-quantitative abundances (>5%, > 50 grains). Data for other W indicators—e.g., Mo, As, Bi, Be—were lacking and not considered in the scoring process. To limit false positives and false negatives resulting from sampling bias, only the highest score from these geochemical and mineralogical subsets was used. Certainty of potential was estimated by ranking each dataset on a scale of 2–5. The HMC mineralogy dataset provided the least certainty (i.e., rank 2), and the ARDF dataset provided the most (i.e., rank 5). The overall certainty score for a given HUC is the sum of the certainty ranking of ARDF and the certainty ranking of whichever geochemical or mineralogical dataset contributed to potential score for the HUC. The Supplementary Data C section shows the detailed scoring parameters for potential and certainty.

4.5. Quantitative assessment and economic filtering

The quantitative portion of this work applies the last phase of the three-part form of assessment that uses expert estimates at the 90th, 50th, and 10th percentiles to produce a probability distribution of the number of undiscovered deposits that may be present in the tract along with quantitative and economic resource analysis. In MapMark4, Monte Carlo simulation is then used to combine the distribution of undiscovered deposits with grades and tonnages from the global grade and tonnage model to produce a probability distribution of the amount of contained metal in the tract. Finally, in addition to the determination of regional resource potential, this quantitative assessment applies the recently developed Resource Assessment Economic Filter (RAEF; Shapiro and Robinson, 2019), a graphical user interface tool that applies a set of mine cost equations to the undiscovered deposits, to constrain the value of undiscovered resource that may be economically recoverable. The assessment team concluded that only the western YTU sub-tract (see Section 5.1) was sufficiently data rich to warrant quantitative assessment.

The total number of undiscovered deposits in a permissive tract is estimated through the Delphi-expert elicitation method. For the purposes of this study, a 'deposit' is a site with a well-characterized mineral resource estimate, whose size and grade falls within the range of deposits in the global W skarn grade and tonnage model (Green et al., 2020). Deposits that are 'unknown' or 'undiscovered' can include deposits that have yet to be discovered, as well as known prospects and

occurrences that may be upgraded to deposits through additional drilling and resource delineation. A total of 20 USGS geologists, all involved in assessing W skarn potential in areas across the U.S., provided estimates of numbers of undiscovered deposits <500 m below the surface at levels of certainty of 90%, 50%, and 10%. To make the estimates of undiscovered deposits in the tract, the geologists evaluated the geologic map, stream sediment chemistry, pan concentrate mineralogy, and known mineral sites. After a preliminary round of estimations, the geoscientists discussed key factors that went into their estimations and a second (final) round of estimations was made. For statistical purposes, the most weight (1) was given to estimates from those individuals with more first-hand experience studying the geology of eastern Alaska and those with extensive experience in quantitative assessments; estimates of the others received a weight of 0.5. Using the MapMark4 R package (Ellefsen, 2017a, 2017b), these estimates were used to derive a negative binomial probability mass function of undiscovered deposits. A negative binomial distribution is assumed because of the discrete nature of the data.

To quantify a probabilistic range of the amount of undiscovered resource that may be present, a Monte Carlo simulation ($n = 20{,}000$) is executed in the MapMark4 computer program with the grade and tonnage model and expert estimates as inputs (Ellefsen, 2017a, 2017b). Based on the probability distribution of the number of undiscovered deposits, the simulation randomly samples the global grade and tonnage model to generate a probability density distribution of total ore tonnages and contained WO_3 that may be present in the tract.

Cost of mining, metal prices, and other factors must be considered to realistically estimate the economic value of in-ground undiscovered resources in a tract. We used the Resource Assessment Economic Filter (RAEF), a R software package designed to provide an economic filter of undiscovered mineral resource estimates by using mine, mill, and mine waste cost models appropriate for the deposit type under consideration. The Monte Carlo simulation results derived from MapMark4 provide the input for the RAEF program (Singer and Menzie, 2010; Ellefsen, 2017a, 2017b; Shapiro, 2018). The software algorithms and default parameter values for RAEF are discussed in detail in Shapiro and Robinson (2019). Certain mining and economic factors are assumed to apply to any potential W skarn mines in the study area (Table 3), namely, the use of a flotation mill and tailings pond and dam with liner, and ~ 350 day/yr operation. It is also assumed that potential undiscovered deposits are evenly distributed down to the assessment depth of 500 m and that orebodies deeper than 60 m will be mined via underground methods. The economic Marshall-Swift cost updating index, the composite of changes in raw material, energy, labor, and construction costs for the mining industry, and investment rate of return parameters are set to their default values (Shapiro and Robinson, 2019) as no foreseen shift in cost are considered for the area. Based on recommendations made by Green et al. (2020), the 20-year average commodity value for WO_3 is $26,500 (2008 dollars), and a typical metallurgical recovery rate for the flotation process is assumed to be 75%.

Table 3
RAEF analysis parameters (see Shapiro and Robinson, 2019, for step by step method and definitions).

	Best Case	Worst Case
Morphology	Massive/Disseminated	Steep
CCIF	1	1.8
OCIF	1	1.5
Mill Type	Flotation	
Days of Operation	350	
Waste Management	Tailings pond and dam	
Liner	Yes	
MSC	1.26	
IRR	0.15	
Commodity Value	$26,500	
MRR	0.75	

CCIF = Capital cost inflation factor
OCIF = Operating cost inflation factor
MSC = Marshall-Swift cost index
IRR = Investment rate of return
MRR = Metallurgical recovery rate

Mining and economic factors in RAEF that may vary within the tract or between possible deposits are the orebody morphology and capital and operating cost inflation factors. The morphology of a W skarn orebody may vary depending on the composition and volume of the host rocks and the presence of pre- or post-mineralization structures controlling the orientation of the ores. The RAEF program can model, in order from least to most costly, the following: massive/disseminated ores, flat-lying/stratabound ores, or steeply dipping ores. The capital cost inflation factor (CCIF) and operating cost inflation factor (OCIF), when set higher than their default value of 1, are unitless inflation factors designed to reflect the higher costs of building and operating a mine in remote areas such as Alaska. For instance, an OCIF value of 1.5 simulates 50% higher operating costs that may be incurred for onsite accommodation, more expensive energy and fuel, and product transportation.

5. Results

5.1. Descriptions of permissive tracts

Three distinct permissive sub-tracts are defined within the study area that contain the requisite rock types. For the Yukon-Tanana Upland (YTU), these are defined as the 1) Western YTU, 2) Eastern YTU, and 3) Southern YTU (Fig. 6; Table 4), which have distinctive geologic and metallogenic features.

The Eastern YTU sub-tract begins at the western edge of the Charley River, Eagle, and Tanacross quadrangles and extends to the U.S-Canada border. Outcropping rocks are arc and basinal assemblages of the allochthonous Yukon-Tanana terrane (YTT; Figs. 4, 6). Although geochemical data are available, this tract has the sparsest concentration of sampling of the three tracts. This is the only tract to contain Jurassic-age intrusive rocks (Fig. 4). These differences in data quality and rock types warranted a separate sub-tract.

The Southern YTU tract is located south of the Alaska Highway in the northern portion of the Alaska Range (Fig. 6). Although this tract is within a distinct geographic terrane, the rocks are like those found in the Western YTU (Fig. 4). However, mapped Cretaceous plutons are much less prevalent than in the YTU north of the highway. Base metal and Au skarn occurrences within this geographic province are reported in the ARDF data, but not within the tract itself. We attribute this inconsistency to the combined reconnaissance-scale mapping in the area and limited data in some ARDF reports.

The Western YTU sub-tract includes the Fairbanks and Circle quadrangles and their major placer gold-mining districts. This tract encompasses parautochthonous assemblages of the YTU that have been intruded by middle Cretaceous to Tertiary pulses of granitic plutons (Figs. 3, 4). The western and northern parts of the Western YTU sub-tract have been extensively explored for a variety of commodities. Consequently, the tract has the highest density of available geochemical data. The only historical W production in the Alaska side of the YTU occurred at Gilmore and Mastadon Domes, near Fairbanks (Table 1; Fig. 6). The Western YTU sub-tract includes tracts defined by Menzie et al. (1983), but also identifies additional permissive ground in the Circle quadrangle and elsewhere in the adjacent quadrangles (Fig. 6).

5.2. Qualitative assessment

The W skarn mineral potential map of the YTU is shown in Fig. 7. The procedure successfully identifies high potential in parts of the tract where there are known W skarn or related W-bearing mineral sites, including the Fairbanks district (FD), Table Mountain (TM), and Weston (Fig. 7). It also identifies high potential in areas where such W-bearing

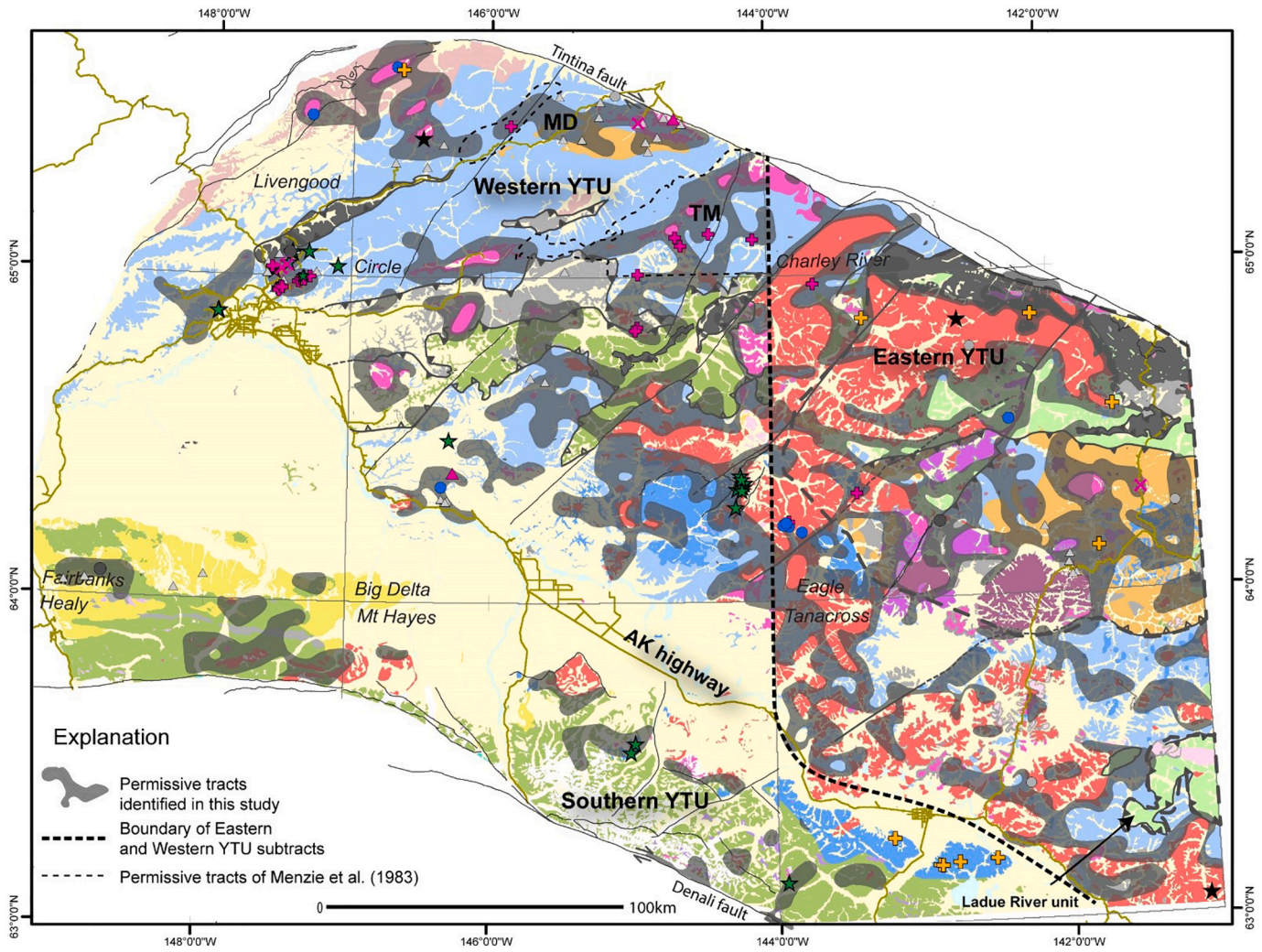

Fig. 6. Map of permissive tracts (based on proximity of carbonate-bearing rocks and felsic granitoids) shown as transparent gray overlain on regional geology modified from Wilson et al. (2015) and Dusel-Bacon et al. (2017). General boundaries of tract subdivisions are based on a combination of lithotectonic and data quality boundaries. The Western/Eastern YTU boundary follows the western border of the Charley River-Eagle-Tanacross boundaries, as these quadrangles have far less data available and are dominated by allochthonous rocks. Supplementary Data A and B describe the search terms and smoothing/aggregation methods used in tract creation. Mineral site symbology from Fig. 1. And geology from Fig. 4. MD - Mastodon Dome, PG - Puzzle Gulch.

Table 4
Geologic characteristics of the permissive sub-tracts.

Sub-tract	Area (km^2)	Lithotectonic Packages	Plutonism	Notable W mineral sites	Historic WO_3 Production	Geochemical data	Mineralogical data	Assessment type
Western YTU	9200	Lower plate / parautochthon - Fairbanks/Chena assemblages, Totatlanika schist and equivalents	middle Cretaceous to early Tertiary	Gilmore Dome; Table Mountain; Puzzle Gulch	40 t	Quantitative and semi-quantitative	Available	Quantitative
Eastern YTU	11,100	Upper plate / allochthon - Fortymile assemblage; Lower plate / parautochthon - Lake George, Ladue River assemblages	Triassic to early Tertiary	Lucky 13; Duval Creek	none	Mostly semi-quantitative	Absent	Qualitative
Southern YTU	2100	Lower plate / parautochthon - Butte assemblage, Jarvis belt, Totatlanika schist and equivalents	Sparse; Late Cretaceous to early Tertiary	None, but other skarn types present - Peak and Eagle	none	Quantitative and semi-quantitative	Available	Qualitative

deposits have not been documented (e.g., Napoleon Creek (labeled NC); Fig. 7). In general, drainage areas characterized by at least one high stream sediment geochemical/mineralogical anomaly and a known mineral site scored high mineral potential and high certainty, whereas drainage areas with only high stream sediment anomalies scored high potential and medium certainty.

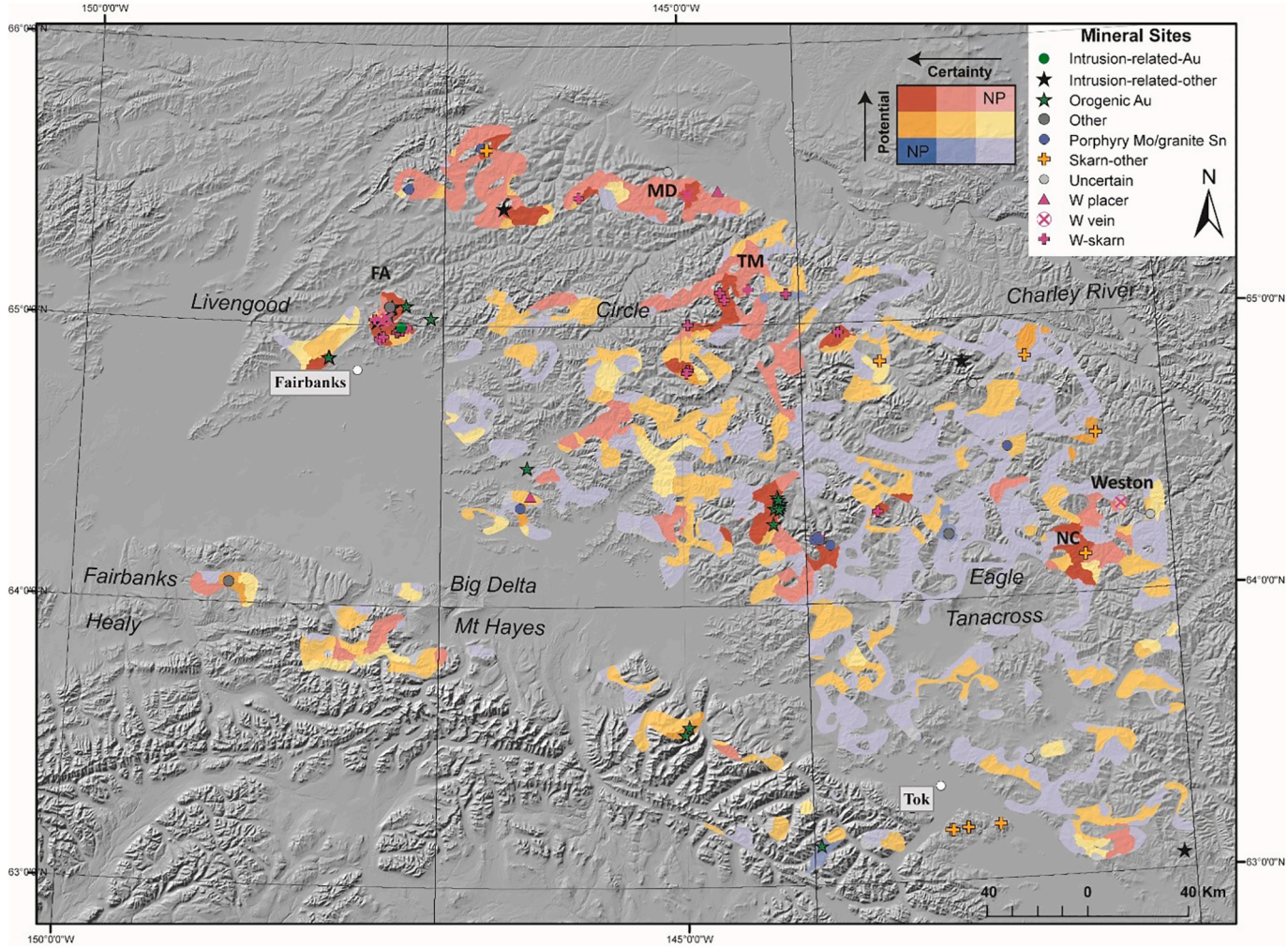

Fig. 7. Permissive tracts (from Fig. 6) showing HUC-based mineral potential mapping scores applied and overlain on a DEM and also showing ARDF deposit and occurrence locations with reported elevated tungsten (W). See Supplementary Data C for scoring protocol. NP – not present, TM – Table Mountain, MD – Mastadon Dome, FA, Fairbanks area. DEM data from U.S. Geological Survey (2020b) and Government of Yukon and Natural Resources Canada (2006).

The Western YTU sub-tract has the highest concentration of high mineral potential HUCs, and notably contains more HPMC drainage areas than the Eastern YTU sub-tract (Fig. 7). This likely reflects both the change in tectonic assemblages (parautochthonous North America versus YTT strata; Fig. 4) and significantly sparser data coverage in the Eagle quadrangle. The portion of the permissive tract trending east-west across the middle of the Circle quadrangle is characterized by consistently high mineral potential scores but lacking known W skarn sites. This tract encompasses the Lime Hill and Circle Hot Springs granitic complexes (Foster et al., 1983), which are associated with multiple Sn—W greisen and Sn—W skarn mineral sites, indicating a favorable mineral system environment for W skarn mineralization.

Although permissive tracts in the southern YTU lack known W skarn sites and are of limited spatial extent, most received medium to high scores for W skarn potential (Fig. 7). The presence of other types of skarn systems in this belt, including the economically significant, but much younger (~70 Ma), Peak Au deposit (Illig, 2015), suggests a favorable environment for skarn formation. Interestingly, no permissive tracts are in the vicinity of Peak. This is most likely because the causative intrusion is not exposed close to the deposit and is inferred to be at depth. Indeed, few intrusive bodies are mapped in the area, and it is unclear if suitable types are present. More robust U/Pb geochronology and geochemical data are needed in this area to delineate the extent of the 100–90 Ma plutons that are associated with W skarn mineralization elsewhere in the region.

5.3. Quantitative probabilistic estimates of undiscovered resources

The individual expert estimates of undiscovered deposits in the ca. 9200 km^2 Western YTU sub-tract are shown in Table 5. Rationale employed by the expert panel for indicating that the tract is favorable include favorable lithology, previous production, clustering of previously mined deposits, W placers in the area, lack of recent exploration, pan concentrates containing W-bearing minerals, and W geochemical anomalies. Uncertainties and negative characteristics making the tract unfavorable are addressed in Section 6. The distribution suggests that the highest relative probability ($p = 0.26$) is for the presence of two undiscovered deposits (point A; Fig. 8). Cumulative relative probability is $p = 0.7$ for one to three undiscovered deposits to be present in the permissive tract; the probability of no deposits is 0.1 (points B and C, respectively; Fig. 8). By comparison, Menzie et al. (1983) estimated one to two undiscovered W skarn deposits in their Circle quadrangle tracts at the 50 and 10 probability percentiles, respectively. Extrapolating their estimates to the rest of the Western YTU suggests that the estimates are slightly more conservative.

Based on the MapMark4 Monte Carlo simulation, the total contained ore tonnage for the tract spans orders of magnitude from P90 = 622 kt, to P50 (median) = 20,200 kt, to P10 = 68,900 kt. The total contained WO_3 tonnage ranges from P90 = 2 kt, P50 = 94 kt, to P10 = 350 kt (Table 6; Fig. 9). The upper limit is comparable to the contained WO_3 at Mactung (Table 1). Due to the considerable uncertainty of the expert

Table 5
Individual expert estimates of undiscovered deposits.

Estimator	Weight	Estimation		
		90%	50%	10%
1	1	1	2	3
2	1	0	1	3
3	1	2	3	5
4	1	0	1	2
5	1	1	2	2
6	0.5	1	3	5
7	0.5	0	1	2
8	0.5	1	2	3
9	0.5	1	2	3
10	0.5	2	4	5
11	0.5	2	5	10
12	1	1	3	5
13	1	1	2	7
14	1	2	4	6
15	1	2	2	3
16	0.5	1	1	3
17	0.5	1	2	4
18	0.5	2	3	5
19	0.5	1	3	7
20	0.5	1	2	3

estimations, total contained ore and metal at the 99th percentile is 0. This does not mean the tract contains no undiscovered W skarn ore; rather, it means that the tract may not contain W skarn ore of sufficient size to constitute a deposit in the global grade and tonnage model. Overall, the quantitative assessment results yield a geologically reasonable range of undiscovered W resource in the study area in the context of W skarn districts elsewhere in the Cordillera and suggest that the Western YTU tract area is prospective for hosting significant W skarn deposits.

5.4. Economic filtering

For this study, we applied best-case and worst-case scenario economic filters in RAEF to encompass the range of mining scenarios that might apply to the Yukon-Tanana Upland based on variations in the location and morphology of the orebody (Table 3). The economic dollar value of the tract after mining costs and investment return rates are considered is represented as net present value (NPV) as defined in Shapiro and Robinson (2019).

In this exercise, the best-case scenario is a disseminated orebody located near Fairbanks, close to existing infrastructure and power sources; the CCIF and OCIF values are set to their default of 1. Given the historical W production from the Gilmore Dome, such a scenario is geologically possible. The worst-case scenario is a steeply dipping orebody located far from Fairbanks and major roads. In such a scenario, capital costs would be much higher (CCIF = 1.8) due to the need to build access roads, a powerplant, and other infrastructure, and operating costs (OCIF = 1.5) would also be increased due to higher energy, transportation, and onsite accommodation costs. The steep orientation of the orebody limits mining to the vertical crater retreat method, a type of stope mining (Hamrin, 2001). Fig. 10A shows the range of simulated undiscovered deposits that remain economically recoverable in the best-case and worst-case scenarios. In the best-case scenario, median recoverable WO_3 is 63 kt and most simulated deposits and all known deposits in the grade and tonnage model are economic. The median NPV of undiscovered W resource in the tract is ~$330,000,000 (Table 7). In the worst-case scenario, deposits smaller than 3000–5000 kt of ore and ~ 0.39–0.43% WO_3 are unlikely to be economic (Fig. 10A). Median recoverable WO_3 is 30 kt, and the NPV is only $44,000,000. The morphology of the orebody has little effect on the NPV of undiscovered deposits above the 50th percentile (Fig. 10B). An appreciable difference is only noted between disseminated orebodies and flat-lying and steep orebodies at probabilities <20–30%, where tonnages increase

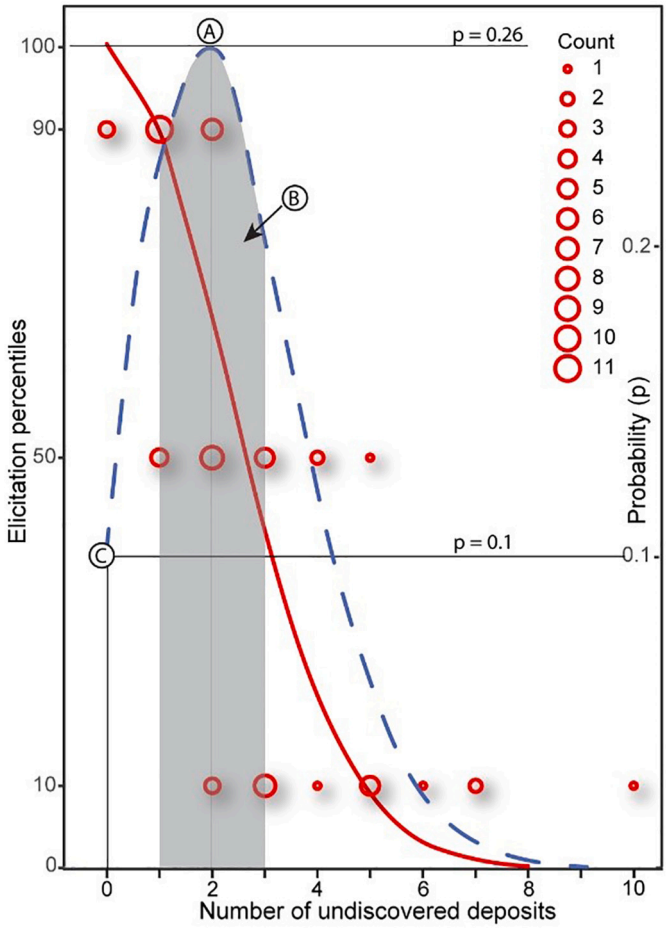

Fig. 8. Probability distribution (blue dashed line) and percentiles (red solid line) of undiscovered deposit estimations in the Western YTU sub-tract. Open red circles show the total elucidated counts for each number of undiscovered deposits. A) Shows the highest probability (p = 0.26, 2 undiscovered deposits), based on expert estimations. B) The shaded (cumulative) area comprising 70% probability of one to three undiscovered deposits in the Western YTU sub-tract. C) Statistical modeling indicates a 10% likelihood ($p = 0.1$) of no deposits that fall within the range of the global grade-tonnage model. (For interpretation of the references to colour in this figure legend, the reader is referred to the web version of this article.)

Table 6
Summary statistics of MapMark4 Monte Carlo simulation of total undiscovered resources in the western YTU tract.

	Ore resource (kt)	Contained WO_3 (kt)
Mean	28,800	143
Maximum	207,300	1600
Minimum	0	0
Median	20,200	94
Std. Dev.	28,400	156
P99	0	0
P90	622	2
P80	4600	20
P70	9030	40
P60	14,200	64
P50	**20,200**	**94**
P40	27,600	128
P30	37,100	175
P20	49,800	242
P10	68,900	350
P1	120,000	701
Prob. of Zero	0.10	0.10
Prob. ≥ Mean	0.39	0.37

Median (P50) values bolded.

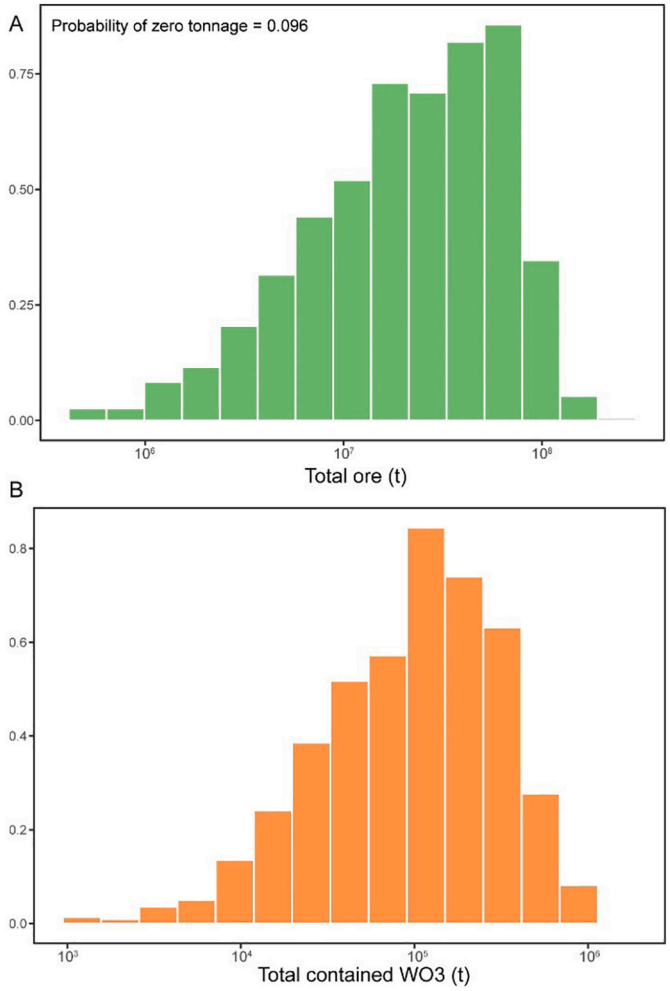

Fig. 9. Density plots of total Western YTU sub-tract resources simulated in MapMark 4. A) Total ore tonnage. B) Total contained WO_3 tonnage.

dramatically. There is almost no difference in NPV between flat-lying and steep orebodies, except in the high CCIF and OCIF scenario.

To summarize, assuming other mining and market economic factors are the same for all possible undiscovered deposits in the tract, the RAEF analysis indicates that proximity to infrastructure is the most important factor controlling economic value of an undiscovered deposit; orebody morphology is less important.

6. Discussion

6.1. Sources of uncertainty

Identifying sources of uncertainty and bias in the qualitative and quantitative resource assessment approach is important for guiding stakeholder decision-making and revealing knowledge gaps that warrant further study. Empirical uncertainties in this assessment can be grouped into two categories: uncertainties in the mappable criteria datasets used to generate the permissive tracts, and uncertainties in ground-truthing the presence of W skarn mineralization; both can result in false negatives or false positives. The coarse mapping resolution and poor exposure in the study area result in overgeneralization of the geologic mappable criteria and possible omission of small granitic plutons and carbonate roof pendants—the latter of which may be highly prospective for being mineralized. While omission can result in false negatives, map generalization can also result in false positives. For instance, in the study area, the actual spatial extent of carbonate-bearing horizons grouped into a mapped unit may be limited, and not all granitic intrusions may have favorable compositions. Primary mapping errors (i.e., inaccurate contacts) are an additional source of uncertainty, but at the 1:250,000 scale, they are not likely to impact the permissive tracts.

Uncertainties in indicators of mineralized bedrock encompass stream sediment mineralogy and geochemistry and the mineral site database. Historically, mineral identification has been visual, and both subjective and qualitative. Censoring of geochemical data may result in false negatives, particularly for methods with high DLs; conversely, determinations close to those high DLs can result in false positives. Additionally, sparse coverage of the geochemical datasets limits the ability to ground-truth potential in many areas that are otherwise geologically permissive. Owing in part to remoteness and limited W-focused exploration in the region, the significance of known W skarn sites in the region is uncertain. Most of the W skarn mineral sites outside of the Gilmore Dome area lack detailed geologic descriptions, drilling, or other indicators of potential size and grade. Overall, the study area is considerably less well explored for W than other Cordilleran districts in Canada and the conterminous U.S.

The extent and certainty of future assessments would be substantially improved by increasing the 3-D coverage and quality and coverage of geological, geochemical, geophysical data across the Yukon-Tanana Upland. In particular, reanalyzing legacy geochemical samples via modern total decomposition and ICP-MS methods would greatly reduce both false positives and negatives due to high analytical method detection limits and partial decomposition techniques in the legacy data. Higher-resolution aeromagnetic and gravity geophysical data would reduce uncertainty caused by coarse geologic mapping resolution and increase geologic knowledge in the third dimension by identifying, for example, subsurface extensions of permissive tracts and previously unmapped intrusions.

In addition to empirical uncertainties, conceptual uncertainties in the understanding of the intrusion-related mineral system reduce certainty in estimates of undiscovered W skarn deposits. More research is needed to constrain the processes that ultimately control magma compositions in the Yukon-Tanana Upland and Canadian Cordillera. Whereas geochemically distinct suites of evolved and reduced intrusions have been identified and correlated with W skarn mineralization, the underlying source regions of these melts and how they differ from those of more oxidized and less evolved Cu-Au-Mo porphyry systems in the region is not entirely clear. It is possible that the melts were derived from, or interacted with, distinct lithotectonic packages.

From the broader mineral system perspective, considerable knowledge gaps remain in the understanding of ore forming processes in other types of W-bearing systems—primarily intrusion-related Au and orogenic Au. An initial goal of this study was to assess potential in the YTU for W-bearing variations of these Au system types in addition to W skarn, as they may provide byproduct sources of W. For example, Fort Knox is known to have locally high enrichments of W in the Au orebody and adjacent skarn (D. Poole, pers. comm., 2019). However, it became clear early on that the geologic understanding of W in these systems was too limited to derive mappable criteria specific to the W-rich systems. This is in part because the factors that govern W enrichment in orogenic systems have not been extensively studied outside of the Otago district in New Zealand (Cave et al., 2017). Furthermore, little work has investigated the genetic relationships between the W skarns of the Gilmore Dome and Au mineralization in the Fort Knox deposit implied by the reduced intrusion-related gold model (Hart, 2005, 2007). More robust U/Pb geochronology data are needed to establish W skarn mineralization ages at Stepovich and Yellowpup. Existing K/Ar and Ar/Ar age determinations of alteration minerals from these deposits reflect cooling ages, not the time of mineralization. Age determinations are up to 5 myr younger than the 91 Ma *Re*—Os (molybdenite) mineralization age of Fort Knox (Allegro, 1987; Selby et al., 2002). Consequently, a definitive temporal link between W skarn and Au mineralization timing has yet to be determined.

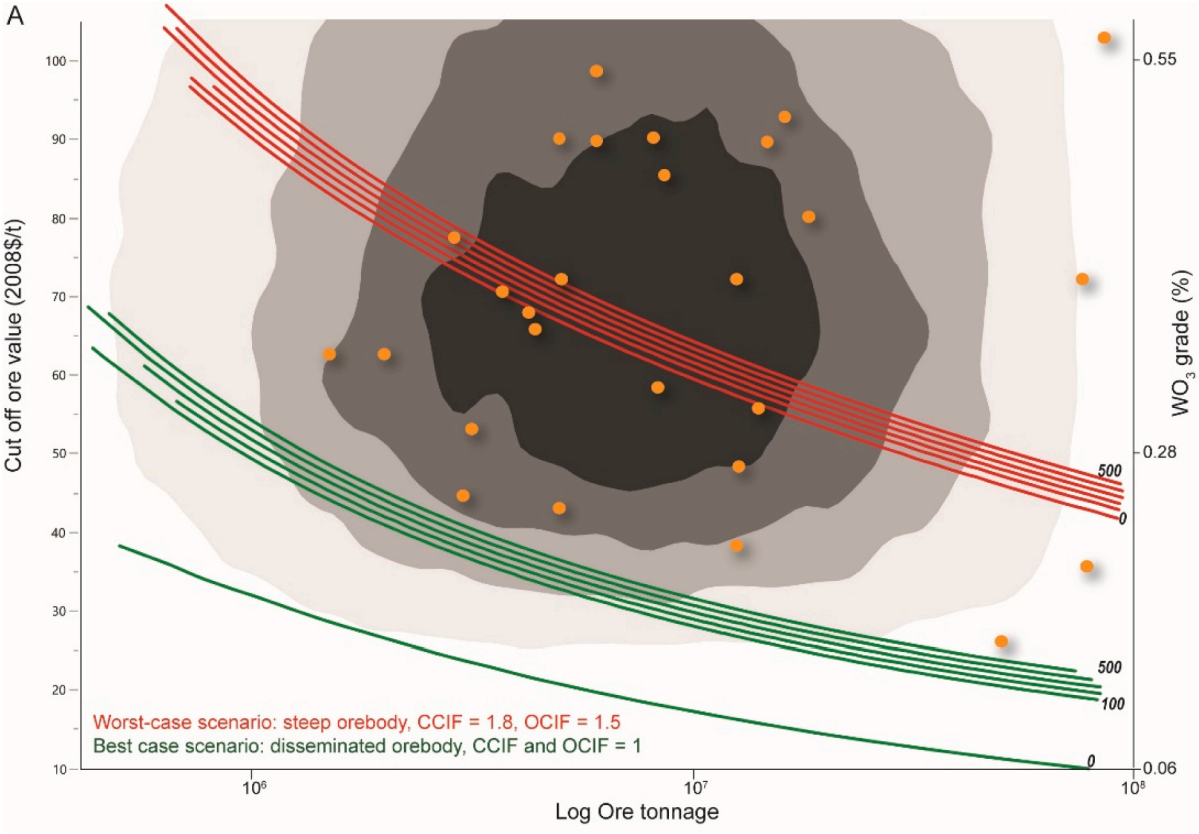

Fig. 10. A) Density plot of Map Mark 4 simulated ore tonnages and values (grades); $n = 20{,}000$. The economic cutoffs of the best- and worst-case scenarios are shown in green and red, respectively. Orange dots are known deposits on the grade-tonnage model. Adapted from RAEF diagram output. B) Probability curves of total tract NPV calculated in RAEF for different economic and orebody morphology scenarios. (For interpretation of the references to colour in this figure legend, the reader is referred to the web version of this article.)

The role of estimator bias in the quantitative assessment must also be considered. Sources of bias include area of expertise, level of experience in conducting assessments, and extent of knowledge and work experience in the study area. Although such biases cannot be eliminated, several aspects of our approach help mitigate them. First, the assessment utilized elicitation of estimates from a large group of geoscientists ($n = 20$; Table 5). The iterative nature of the assessment, including discussion, enhanced the assessors' broader understandings of the geological characteristics of the assessment area. Finally, the weighting accounted for the geoscientists' relative experience in eastern Alaska geology and/or mineral resource assessments.

6.2. *Comparisons of potential in other W skarn districts*

The range of NPV of $44 to $330 million of the entire Western YTU sub-tract is comparable to that of the similarly remote Mactung ($250 million; Narciso et al., 2009) and Watershed ($110 million; Queensland, Australia; Iannucci, 2017) deposits, suggesting that the simulated NPV range in the Western YTU is reasonable. This assessment of W skarn deposit potential in eastern Alaska carries implications for deposit estimation throughout the North American Cordillera. Preliminary quantitative assessments in the Idaho-Montana Great Falls tectonic zone (GFTZ; Andersen et al., pers. comm., 2020) and Great Basin (GB; USGS Great Basin Tungsten Assessment Team, pers. comm., 2020) regions of the Cordillera by the same assessment team yielded significantly higher

Table 7
Summary statistics of the RAEF analysis. The abbreviations should all be defined.

	Best Case Scenario		Worst Case Scenario	
	Recoverable WO_3 (kt)	NPV (million$)	Recoverable WO_3 (kt)	NPV (million$)
Mean	98	575	70	220
Maximum	1161	8134	1100	5265
Minimum	0	0	0	0
Median	63	329	30	44
Std. Dev.	110	708	100	386
P99	0	0	0	0
P90	0	0	0	0
P80	10	29	0	0
P70	25	107	0	0
P60	42	204	0	0
P50	**63**	**329**	**30**	**44**
P40	87	482	53	109
P30	120	683	83	209
P20	167	998	131	370
P10	244	1503	204	677
P1	492	3165	438	1836
Prob. of Zero	0.15	0.15	0.40	0.40
Prob. ≥ Mean	0.36	0.35	0.34	0.29

NPV – Net Present Value (2008 dollars), P99–99% probability.
Median (P50) values bolded.

estimates of undiscovered W skarn deposits and contained W resources. Median WO_3 t•km^{-2} in the Western YTU tract is ~10—much lower than the GFTZ (~25) and GB (~17). This difference in estimated contained WO_3 reflects interpretations of fundamentally different regional geology as well as degree of historical exploration and assessment certainty. Although W has been less explored in the eastern Alaska study area compared to the western U.S., exploration to date for W and other commodities has revealed few discoveries aside from the Gilmore Dome, and this contributed to low undiscovered deposit estimates.

Geologic differences are considerable. While W skarn-forming Cretaceous magmatic suites are present throughout the Yukon, British Columbia, and the western U.S., the country rocks they intrude vary, which may impact the volume, continuity, and quality of trap/sink rock for mineralizing fluids. Increasing metamorphic grade prior to intrusion may reduce rock permeability and drives differential strain between carbonates and siliciclastic rocks that may dismember continuous horizons. This appears to be the case in the study area, where regionally continuous carbonate horizons are uncommon. In contrast, the Cantung (10.8 Mt. @ 1.2% WO_3) and Mactung (44.9 Mt. @ 0.85% WO_3) deposits in Canada (Table 1) and Browns Lake (6.03 Mt. @ 0.55% WO_3; GFTZ) and Pilot Mountain (12.5 Mt. @ 0.27% WO_3; GB) deposits in the U.S. (Green et al., 2020) are typified by rocks of greenschist or lower metamorphic grade and greater regional continuity. In the latter two districts, the country rocks are effectively flat lying, thick (>6 km), and unmetamorphosed. We can only speculate that this may explain the differences between geologic favorability of the YTU and other regions, as it is beyond the scope of this study to evaluate the relationship between regional metamorphic grade and deposit size for W skarns. Regardless of differences in estimated resources between districts, the YTU remains prospective for undiscovered W skarn deposits.

7. Conclusions

The last decade has witnessed a growing need for explorationists, academics, and government policymakers to improve understanding of the geology and potential availability of critical mineral resources. Tungsten (W) has many industrial and military applications and is one of the few critical minerals that can currently be mined as a primary product. Consequently, the qualitative and quantitative methods incorporating the USGS three-part form of assessment can be a useful tool to estimate potential for undiscovered W deposits where the requisite data exist.

Application of the three-part method to the geologically complex Yukon-Tanana Upland (YTU) region of the North American Cordillera, utilizing an updated W skarn grade-tonnage model and digitized geologic and geochronology datasets, enabled delineation of permissive tracts for W skarn deposits across the uplands. Qualitative assessment of the permissive tract revealed high mineralization potential and data quality in sub-tracts within parautochthonous rocks of the western uplands. This area was then quantitatively assessed and estimates by 20 experts suggest there may be between one to three undiscovered W skarn deposits in this tract at the 70% cumulative probability percentile. A probabilistic Monte Carlo simulation ($n = 20{,}000$), based on the expert estimates and grade and tonnage model, suggests a range of total undiscovered WO_3 in the tract to be from 2 kt, to 94 kt, to 350 kt at the 90%, 50%, and 10% probability percentiles, respectively. Using the USGS Resource Assessment Economic Filter, the median ($P = 50\%$) total economically recoverable WO_3 is 63 kt and the NPV of the tract is $330 million USD (2008 dollars) in a best-case scenario in which the undiscovered deposits are located close to infrastructure. In contrast, median recoverable WO_3 is only 30 kt and the NPV is $44 million in a worst-case scenario in which the deposits are distal to infrastructure.

The simulated potential size ranges of undiscovered deposits in the YTU are geologically reasonable and comparable to the Cantung or Mactung deposits, but the contained WO_3 resource and NPV estimates of the YTU are significantly less than concurrent estimates made in W skarn districts in the contiguous U.S. and known resources in the Yukon and Northern Territories. We speculate that the difference may be explained in part because of relatively high uncertainties in the input datasets as well as variations in major geologic controls—specifically, decreased permeability and continuity of favorable carbonate rock horizons in the relatively higher metamorphic grade of host rocks in the uplands. However, other geologic factors such as regional magma petrogenesis and fertility may play a role. More modern geochemistry, geophysics, and geologic mapping, especially in the third dimension, are necessary to improve empirical uncertainties in this and future assessments. Nevertheless, the USGS three-part mineral resource assessment is still a useful tool for making first-order regional estimates of undiscovered resources and steering research on the fundamental controls of district-scale metallogenic budgets.

Declaration of competing interest

The authors declare that they have no known competing financial interests or personal relationships that could have appeared to influence the work reported in this paper.

Acknowledgements

This research was funded by the U.S. Geological Survey (USGS) Mineral Resources Program (MRP). The authors acknowledge the contributions of participants of the USGS MRP's Mineral Resource Assessment Training participants, including Graham Lederer, Heather Parks, Allen Andersen, Connie Dicken, Carma San Juan, Celeste Mercer, Damon Bickerstaff, Federico Solano, Josh Coyan, Kathryn Watts, Kevin Denton, Maggie Goldman, and Mitchell Bennett. The authors also acknowledge Michael Zientek, Jane Hammarstrom, Keith Long, Gilpin Robinson, Mark Mihalasky, and Mikki Johnson. The authors thank the anonymous reviewers for insightful comments that greatly improved the manuscript. Any use of trade, product, or firm names is for descriptive purposes only and does not imply endorsement by the U.S. Government.

Appendix A. Supplementary data

The Supplementary Data A section lists search keywords for

extraction of permissive rock types from the Geologic Map of Alaska. The Supplementary Data B section describes the permissive tract smoothing and aggregation methods. The Supplementary Data C section lists scoring criteria for the mineral potential mapping/qualitative assessment exercise. Attributed tracts in GIS format, along with the Python script used in the mineral potential mapping exercise, are in Supplementary Data D. The supporting data are also available as a U.S. Geological Survey Data Release at doi:https://doi.org/10.5066/P9TDKQE4. Supplementary data to this article can be found online at doi:https://doi.org/10.1016/j.gexplo.2020.106700.

References

Aleinikoff, J.N., Nokleberg, W.J., 1989. Age of deposition and provenance of the Cleary sequence of the Fairbanks schist unit, Yukon-Tanana terrane, east-central Alaska. In: Dover, J.H. (Ed.), Geologic studies in Alaska by the U.S. Geological Survey, 1988: U.S. Geological Survey Bulletin, 1903, pp. 75–83. https://doi.org/10.3133/b1903.

Allegro, G.L., 1987. The Gilmore Dome Tungsten Mineralization Fairbanks Mining District, Alaska. MSc Thesis. University of Alaska Fairbanks (163 p).

Anderson, R.G., 1983. Selwyn plutonic suite and its relationship to tungsten skarn mineralization, SE Yukon and District of MacKenzie. In: Current Research, Part B: Geological Survey of Canada Paper 83-1B, pp. 151–163. https://doi.org/10.4095/109319.

Anderson, D., Baker, D.J., 1986. Recent Developments in the Geologic Understanding of MacTung: Mineral Deposits of Northern Cordillera Symposium, 37, pp. 234–244.

Beranek, L.P., Mortensen, J.K., 2011. The Timing and Provenance Record of the Late Permian Klondike Orogeny in Northwestern Canada and Arc-continent Collision Along Western North America: Tectonics, 30, TC5017. https://doi.org/10.1029/2010TC002849.

Berdahl, R.S., 2004. Core Sampling Project Risby property, Yukon Government: Energy, Mines and Resources YMEP Report Number 2003-057, p. 14. http://data.geology.gov.yk.ca/Reference/95635 (Accessed on 2/2020).

Berman, R.G., Ryan, J.J., Gordey, S.P., Villeneuve, M., 2007. Permian to cretaceous polymetamorphic evolution of the Stewart River region, Yukon-Tanana terrane, Yukon, Canada: P-T evolution linked with in situ SHRIMP monazite geochronology. J. Metamorph. Geol. 25, 803–827. https://doi.org/10.1111/j.1525-1314.2007.00729.

Bonvalot, S., Balmino, G., Briais, A., Kuhn, M., Peyrefitte, A., Vales, Biancale, R., Gabalda, G., Moreaux, G., Reinquin, F., Sarrailh, M., 2012. World Gravity Map. BGI-CGMW-CNES-IRD, 3 Plates. http://bgi.omp.obs-mip.fr/activities/Projects/world_gravity_map_wgm.

Bowman, J., Covert, J.J., Clark, A.H., Mathieson, G.A., 1985. The CanTung E Zone scheelite skarn orebody, Tungsten, Northwest Territories: Oxygen, hydrogen, and carbon isotope studies. Econ. Geol. 80, 1872–1895. https://doi.org/10.2113/gsecongeo.80.7.1872.

British Geological Survey, 2011. Tungsten: British Geological Survey Mineral Profile. https://www2.bgs.ac.uk/mineralsUK/statistics/mineralProfiles.html (Accessed on 10/2020).

Brown, V.S., Baker, T., Stephens, J.R., 2002. Ray Gulch tungsten skarn, Dublin Gulch, central Yukon: Gold-tungsten relationships in intrusion-related ore systems and implications for gold exploration. In: Emond, D.S., Weston, L.H., Lewis, L.L. (Eds.), Exploration and Geological Services Division, Yukon Region, Indian and Northern Affairs Canada, pp. 259–268.

Burisch, M., Gerdes, A., Meinert, L.D., Albert, R., Seifert, T., Gutzmer, J., 2019. The essence of time – fertile skarn formation in the Variscan orogenic belt. Earth Planet. Sci. Lett. 519, 165–170.

Byers Jr., F.M., 1957. Tungsten deposits in the Fairbanks district, Alaska. In: U.S. Geol. Survey Bull. 1024-1, pp. D178–D218.

Cave, B.J., Pitcairn, I.K., Craw, D., Large, R.R., Thompson, J.M., Johnson, S.C., 2017. A metamorphic mineral source for tungsten in the turbidite-hosted orogenic gold deposits of the Otago Schist, New Zealand. Miner. Deposita 52, 515–537. https://doi.org/10.1007/2Fs00126-016-0677-5.

Cox, D.P., 1986. Descriptive model of W skarn deposits. In: Cox, D.P., Singer, D.A. (Eds.), Mineral Deposit Models: U.S. Geological Survey Bulletin, 1693 (55 p).

Cox, D.P., Singer, D.A., 1986. Mineral deposit models. U.S. Geol. Surv. Bull. 1693 (379 p.).

Dawson, K.M., 1996. Skarn tungsten. In: Geology of Canadian Mineral Deposit Types: Geological Survey of Canada, Geology of Canada, 8, pp. 495–502.

Dawson, K.M., Dick, L.A., 1978. Regional metallogeny of the Northern Cordillera: Tungsten and base metal-bearing skarns in southeastern Yukon and southwestern Mackenzie. In: Current Research, Part A, Geological Survey of Canada, Paper 78-lA, pp. 287–292.

Deklerk, R., 2003. Yukon MINFILE 2003 – a database of mineral occurrences. In: Yukon Geological Survey CDROM.

Delaney, B., Bakker, F.J., 2014. Technical Report on the Cantung Mine, Northwest Territories, Canada, North American Tungsten Ltd, NI 43–101 Report (148 p.).

Deloitte Sustainability, British Geological Survey, Bureau de Recherches Géologiques et Minières, Netherlands Organisation for Applied Scientific Research, 2017. Study on the review of the list of critical raw materials. In: Executive summary: European Commission (9 p.).

Desautels, P., Gilles, A., Maunula, T., 2007. Technical Report on Risby Tungsten Deposit, Yukon, Wardrop, Playfair Mining Ltd, Document No. 0752860100-REP-L0001-00. Available online at: https://www.sedar.com/FindCompanyDocuments.do (Accessed on 2/2020).

Dick, L.A., 1980. A Comparative Study of the Geology, Mineralogy, and Conditions of Formation of Contact Metasomatic Mineral Deposits in the NE Canadian Cordillera. Ph.D. thesis. Queen's University, Kingston (473 p.).

Dick, L.A., Hodgson, C.J., 1982. The MacTung W-Cu (Zn) contact metasomatic and related deposits of the northeastern Canadian Cordillera. Econ. Geol. 77, 845–867. https://doi.org/10.2113/gsecongeo.77.4.845.

Dusel-Bacon, C., Murphy, J.M., 2001. Apatite fission-track evidence of widespread Eocene heating and exhumation in the Yukon–Tanana Upland, interior Alaska. Can. J. Earth Sci. 38, 1191–1204. https://doi.org/10.1139/cjes-38-8-1191.

Dusel-Bacon, C., Csjtey Jr., B., Foster, H.L., Doyle, E.O., Nokleberg, W.J., Plafker, G., 1993. Distribution, facies, ages, and proposed tectonic associations of regionally metamorphosed rocks in east- and south-central Alaska. In: U.S. Geological Survey Professional Paper 1497-C. Available at: https://dggs.alaska.gov/webpubs/usgs/p/text/p1497c.pdf.

Dusel-Bacon, C., Hansen, V.L., Scala, J.A., 1995. High-pressure amphibolite facies dynamic metamorphism and the Mesozoic tectonic evolution of an ancient continental margin, east-central Alaska. J. Metamorph. Geol. 13, 9–24. https://doi.org/10.1111/j.1525-1314.1995.tb00202.x.

Dusel-Bacon, C., Lanphere, M.A., Sharp, W.D., Layer, P.W., Hansen, V.L., 2002. Mesozoic thermal history and timing of structural events for the Yukon-Tanana upland, east-Central Alaska: $^{40}Ar/^{39}Ar$ data from metamorphic and plutonic rocks. Can. J. Earth Sci. 39, 1013–1051. https://doi.org/10.1139/e02-018.

Dusel-Bacon, C., Aleinikoff, J.N., Day, W.C., Mortensen, J.K., 2015. Mesozoic magmatism and timing of epigenetic Pb-Zn-Ag mineralization in the western Fortymile mining district, east-central Alaska: Zircon U-Pb geochronology, whole-rock geochemistry, and Pb isotopes. Geosphere 11, 786–822. https://doi.org/10.1130/GES01092.1.

Dusel-Bacon, C., Holm-Denoma, C.S., Jones III, J.V., Aleinikoff, J.N., Mortensen, J.K., 2017. Detrital zircon geochronology of quartzose metasedimentary rocks from parautochthonous North America, east-central Alaska. Lithosphere 9 (6), 927–952 (GSA Data Repository Item 2017332). https://doi.org/10.1130/L672.1.

Einaudi, M.T., Meinert, L.D., Newberry, R.J., 1981. Skarn deposits. In: Skinner, B.J. (Ed.), Economic Geology, 75th Anniversary Volume, pp. 317–391. https://doi.org/10.5382/AV75.11.

Ellefsen, K.J., 2017a. User's guide for MapMark4—An R package for the probability calculations in three-part mineral resource assessments. In: U.S. Geological Survey Techniques and Methods, Book 7, chap. C14. https://doi.org/10.3133/tm7C14 (23 p.).

Ellefsen, K.J., 2017b. Probability calculations for three-part mineral resource assessments. In: U.S. Geological Survey Techniques and Methods, book 7, chap. C15. https://doi.org/10.3133/tm7C15 (14 p.).

Engebretson, D.C., Cox, A., Gordon, R.G., 1985. Relative motions between oceanic and continental plates in the Pacific Basin. Geol. Soc. Am. Spec. Pap. 206 https://doi.org/10.1130/SPE206 (59 p.).

Fitzpatrick, K., Bakker, F.J., 2011. Technical Report on the Cantung Mine, Northwest Territories, Canada, North American Tungsten Ltd, NI 43–101 Report (155p.).

Fortier, S.M., Nassar, N.T., Lederer, G.W., Brainard, Jamie, Gambogi, Joseph, McCullough, E.A., 2018. Draft critical mineral list—Summary of methodology and background information—U.S. Geological Survey technical input document in response to Secretarial Order No. 3359. In: U.S. Geological Survey Open-File Report 2018–1021. https://doi.org/10.3133/ofr20181021 (15 p.).

Foster, H.L., 1976. Geologic map of the Eagle quadrangle, Alaska. In: U.S. Geological Survey Miscellaneous Investigations I–922 (scale 1:250,000).

Foster, H.L., 1992. Geologic map of the eastern Yukon-Tanana region, Alaska. In: U.S. Geological Survey Open-File Report 92–313 (26 p., 1 pl., scale 1:500,000).

Foster, H.L., Laird, Jo, Keith, T.E.C., Cushing, G.W., Menzie, W.D., 1983. Preliminary geologic map of the Circle quadrangle, Alaska. In: U.S. Geological Survey Open-File Report 83–170-A (30 p., 1 sheet, scale 1:250,000).

Gabrielse, H., Murphy, D.C., Mortensen, J.K., 2006. Cretaceous and Cenozoic dextral orogen-parallel displacements, magmatism, and paleogeography, north-central Canadian Cordillera. In: Haggart, J.W., Enkin, R.J., Monger, J.W.H. (Eds.), Paleogeography of the North American Cordillera: Evidence for and Against Large-scale Displacements: Geological Association of Canada Special Paper 46, pp. 255–276.

Glover, J.K., Burson, M.J., 1986. Geology of the Lened tungsten skarn deposit, Logan Mountains, Northwest Territories. In: Special Volume Canadian Institute of Mine and Metallurgy, 37, pp. 255–265.

Godwin, C.I., Armstrong, R.L., Thompson, K.M., 1980. K-Ar and Rb-Sr dating and the genesis of tungsten at the Clea tungsten skarn property, Selwyn Mountains, Yukon Territory. In: Canadian Institute of Mining Metallurgy Bulletin, 73, pp. 90–93.

Government of Yukon and Natural Resources Canada, 2006. Contours [computer file]. In: Whitehorse, YK: Geomatics Yukon, 2006 (accessed on 3/1/2020). https://library.mcmaster.ca/maps/geospatial/yukon-digital-elevation-data.

Granitto, M., Wang, B., Shew, N.B., Karl, S.M., Labay, K.A., Werdon, M.B., Seitz, S.S., Hoppe, J.E., 2019. Alaska Geochemical Database Version 3.0 (AGDB3)—including "best value" data compilations for rock, sediment, soil, mineral, and concentrate sample media. In: U.S. Geological Survey Data Series, 1117. https://doi.org/10.3133/ds1117 (33p.).

Green, C.J., Lederer, G.W., Parks, H.L., Zientek, M.L., 2020. Grade and tonnage model for tungsten skarn deposits—2020 update. In: U.S. Geological Survey Scientific Investigations Report 2020–5085. https://doi.org/10.3133/sir20205085 (23 p.).

Gupta, V., Biswas, T., Ganesan, K., 2016. Critical Non-fuel Mineral Resources for India's Manufacturing Sector: Department of Science and Technology, Government of India (104p.).

Hall, M.H., 1985. Structural Geology of the Fairbanks Mining District, Central Alaska: University of Alaska Fairbanks (M.S. thesis, 66 p., charts, illust. (some color)).
Hamrin, H., 2001. Underground mining methods and applications. In: Hustrulid, W., Bullock, R.L. (Eds.), Underground Mining Methods: Engineering Fundamentals and International Case Studies, SME, pp. 3–14.
Hansen, V.L., Dusel-Bacon, C., 1998. Structural and kinematic evolution of the Yukon-Tanana upland tectonites, east-central Alaska: a record of late Paleozoic to Mesozoic crustal assembly. Geol. Soc. Am. Bull. 110, 211–230. https://doi.org/10.1130/0016-7606(1998)110<0211:SAKEOT>2.3.CO;2.
Hart, C.J.R., 2005. Classifying, distinguishing and exploring for intrusion-related gold systems. In: The Gangue: Newsletter of the Geological Association of Canada Mineral Deposits Division, pp. 1–18. https://www.gac.ca/chapters/gangue/Gang87.pdf (Accessed 2/2020).
Hart, C.J.R., 2007. Reduced intrusion-related gold systems. In: Goodfellow, W.D. (Ed.), Mineral deposits of Canada: A Synthesis of Major Deposit Types, District Metallogeny, the Evolution of Geological Provinces, and Exploration Methods: Geological Association of Canada, Mineral Deposits Division, Special Publication No. 5, pp. 95–112.
Hart, C.J.R., Goldfarb, R.J., Lewis, L.L., Mair, J.L., 2004. The northern Cordilleran mid-Cretaceous plutonic province: Ilmenite/magnetite-series granitoids and intrusion-related mineralisation. Resour. Geol. 54 (3), 253–280. https://doi.org/10.1111/j.1751-3928.2004.tb00206.x.
Hu, Z., Gao, S., 2008. Upper crustal abundances of trace elements: a revision and update. Chem. Geol. 253, 205–221.
Hughes, M.A., Siems, P.L., 1980. Lucky 13 Project Area. Union Carbide Corporation, 8 p. (plus plates).
Huskey, G.F., 1981. Lucky 13 Project Area. Union Carbide Corporation (56 p.).
Iannucci, E., 2017. Vital improves watershed economics: Mining Weekly. www.miningweekly.com/article/vital-improves-watershed-economics-2017-09-05 (Accessed 10/20).
Illig, P.E., 2015. Geology and Origins of the Peak Gold-Copper-Silver Skarn Deposit, Tok, Alaska. MSc Thesis. University of Alaska Fairbanks (166 p.).
Jones III, J.V., Karl, S.M., Labay, K.A., Shew, N.B., Granitto, M., Hayes, T.S., Mauk, J.L., Schmidt, J.M., Todd, E., Wang, B., Werdon, M.B., Yager, D.B., 2015. GIS-based identification of areas with mineral resource potential for six selected deposit groups, Bureau of Land Management Central Yukon Planning Area, Alaska. In: U.S. Geological Survey Open-File Report 2015–1021. https://doi.org/10.3133/ofr20151021 (78 p., 5 appendixes, 12 pls. p.).
GIS-based identification of areas that have resource potential for critical minerals in six selected groups of deposit types in Alaska. In: Karl, S.M., Jones III, J.V., Hayes, T.S. (Eds.), 2016. U.S. Geological Survey Open-File Report 2016–1191. https://doi.org/10.3133/ofr20161191 (99 p., 5 appendixes, 12 plates, scale 1:10,500,000).
Kreiner, D.C., Jones III, J.V., Todd, E., Holm-Denoma, C., Caine, J.S., Benowitz, J., 2019. Links between tectonics, magmatism, and mineralization in the formation of Late Cretaceous porphyry systems in the Yukon-Tanana upland, eastern Alaska, USA [ext. abstract]. In: Society of the Geology Applied to Mineral Deposits (SGA), Glasgow, Scotland, August 27–30, 2019 (4 p).
Kwak, T.A.P., 1987. W-Sn skarn deposits and related metamorphic skarns and granitoids. Dev. Econ. Geol. 24 (451 p.).
LaCroix, P.A., Cook, R.B., 2007. Technical Report on the Mactung Tungsten Deposit, MacMillan Pass, Yukon. Prepared for North American Tungsten Corporation Limited by Scott Wilson Roscoe Postle Associates Inc. Report for NI 43-101 (126 p.).
Lennan, W.B., 1986. Ray Gulch tungsten skarn deposit Dublin Gulch area, central Yukon. In: Morin, J.A. (Ed.), Mineral Deposits of Northern Cordillera: The Canadian Institute of Mining and Metallurgy, Special v. 37, pp. 245–254.
Mair, J.L., Hart, C.J.R., Stephens, J.R., 2006. Deformation history of the northwestern Selwyn Basin, Yukon, Canada: Implications for orogen evolution and mid-Cretaceous magmatism. Geol. Soc. Am. Bull. 118, 304–323. https://doi.org/10.1130/B25763.1.
Manuszak, J.D., Ridgway, K.D., Trop, J.M., Gehrels, G.E., 2007. Sedimentary record of the tectonic growth of a collisional continental margin: Upper Jurassic–Lower Cretaceous Nutzotin Mountains sequence, eastern Alaska Range, Alaska. In: Ridgway, K.D., Trop, J.M., Glen, J.M.G., O'Neill, J.M. (Eds.), Tectonic Growth of a Collisional Continental Margin: Crustal Evolution of Southern Alaska: Geological Society of America Special Paper. 431, pp. 345–377. https://doi.org/10.1130/2007.2431(14).
Mathieson, G.A., Clark, A.H., 1984. The Cantung E Zone scheelite skarn orebody, Tungsten, Northwest Territories; a revised genetic model. Econ. Geol. Bull. Soc. Econ. Geol. 79, 883–901. https://doi.org/10.2113/gsecongeo.79.5.883.
Meinert, L.D., 1992. Skarns and skarn deposits. Geosci. Can. 19, 145–162.
Meinert, L.D., Dipple, G.M., Nicolescu, S., 2005. World skarn deposits. In: Economic Geology 100th Anniversary Volume, pp. 299–336. https://doi.org/10.5382/AV100.11.
Menzie, W.D., and Foster, H.L., 1978, Metalliferous and Selected Nonmetalliferous Mineral Resource Potential in the Big Delta Quadrangle, Alaska: U.S. Geological Survey Open-File Report 78-529D, 61 p.
Menzie, W.D., Foster, H.L., Tripp, R.B., Yeend, W.E., 1983. Mineral resource assessment of the Circle quadrangle, Alaska. In: U.S. Geological Survey Open-File Report 83–170-B (57 p.).
Menzie, W.D., Hua, Renmin, Foster, H.L., 1987. Newly located occurrences of lode gold near Table Mountain, Circle quadrangle, Alaska. In: U.S. Geological Survey Bulletin 1682 (13 p. Available at:). https://dggs.alaska.gov/webpubs/usgs/b/text/b1682.pdf (accessed 12/2/20).
Menzie, W.D., Jones, G.M., Elliott, J.E., DeYoung Jr., J.H., Hammarstrom, J.M., 1992. Tungsten—Grades and tonnages of some deposits. In: Contributions to Commodity Geology Research: U.S. Geological Survey Bulletin 1877, pp. J1–J7. Accessed 12/1/20 at. https://pubs.usgs.gov/bul/1877/report.pdf.
Miles, W., Saltus, R., Hayward, N., Oneschuk, D., 2017. Alaska and Yukon magnetic compilation, residual total magnetic field. In: Geological Survey of Canada, Open File 7862, 2017, 1 Sheet. https://doi.org/10.4095/301695.
Miller, M.L., Bradley, D.C., Bundtzen, T.K., McClelland, W., 2002. Late cretaceous through Cenozoic strike-slip tectonics of southwestern Alaska. J. Geol. 110, 247–270.
Misra, K.C., 2000. Skarn deposits. In: Understanding Mineral Deposits. Springer, Dordrecht, pp. 414–449.
Mortensen, J.K., 1992. Pre-mid-Mesozoic tectonic evolution of the Yukon-Tanana terrane, Yukon and Alaska. Tectonics 11, 836–853.
Nabighian, M.N., 1972. The analytic signal of two-dimensional magnetic bodies with polygonal cross-section: its properties and use for automated anomaly interpretation. Geophysics 37, 507–517. https://doi.org/10.1190/1.1440276.
Narciso, H., Iakovlev, I., de Ruijter, M.A., Impey, G., Cowie, S., Tanase, A., Nichols, A., et al., 2009. Amended technical report on the Mactung property. In: North American Tungsten Corporation Ltd. NI-43-101 Report (372 p.).
Nelson, J., Colpron, M., 2007. Tectonics and metallogeny of the British Columbia, Yukon and Alaskan Cordillera, 1.8 Ga to the present. In: Goodfellow, W.D. (Ed.), Mineral Deposits of Canada: A Synthesis of Major Deposit-Types, District Metallogeny, the Evolution of Geological Provinces, and Exploration Methods: Geological Association of Canada, Mineral Deposits Division, Special Publication No. 5, pp. 755–791.
Newberry, R.J., 1982. Tungsten-bearing skarns of the Sierra Nevada. I. The Pine Creek Mine, California. Econ. Geol. 77, 823–844. https://doi.org/10.2113/gsecongeo.77.4.823.
Newberry, R.J., Einaudi, M.T., 1981. Tectonic and geochemical setting of tungsten skarn mineralization in the Cordillera. In: Arizona Geological Society Digest, 14, pp. 99–111.
Newberry, R.J., Swanson, S.E., 1986. Scheelite skarn granitoids: an evaluation of the roles of magmatic sources and process. Ore Geol. Rev. 1, 57–81. https://doi.org/10.1016/0169-1368(86)90005-3.
Newberry, R.J., Smith, T.E., Albanese, M.D., Solie, D.N., Swainbank, R.C., Burton, P.J., Wiltse, M.A., Reifenstuhl, R.R., Pessel, G.H., 1987. Lode mineralization in the Lime Peak-Mt. Prindle area. In: Smith, T.E., Pessel, G.H., Wiltse, M.A. (Eds.), Mineral Assessment of the Lime Peak-Mt. Prindle Area, Alaska: Alaska Division of Geological and Geophysical Surveys Miscellaneous Publication 29F, pp. 7.1–7.81.
Newberry, R.J., Burns, L.E., Swanson, S.E., Smith, T.E., 1990. Comparative petrologic evolution of the Sn and W granites of the Fairbanks-Circle area, interior Alaska. In: Stein, H.J., Hannah, J.L. (Eds.), Ore-Bearing Granite Systems, Pedogenesis and Mineralizing Processes: Geological Society of America Special Paper 246, pp. 121–142.
Newberry, R.J., Layer, P.W., Burleigh, R.E., Solie, D.N., 1998. New 40Ar/39Ar dates for intrusions and mineral prospects in the eastern Yukon-Tanana terrane, Alaska; regional patterns and significance. In: Gray, J.E., Riehle, J.R. (Eds.), Geologic studies in Alaska by the U.S. Geological Survey, 1996: U.S. Geological Survey Professional Paper 1595, pp. 131–159. https://pubs.usgs.gov/pp/1595/.
Nokleberg, W.J., Bundtzen, T.K., Berg, H.C., Brew, D.A., Grybeck, D., Robinson, M.S., Smith, T.E., Yeend, W., 1987. Significant metalliferous lode deposits and placer districts of Alaska. U.S. Geol. Surv. Bull. 1786 (104 p.).
Nokleberg, W.J., Bundtzen, T., Eremin, R.A., Ratkin, V.V., Dawson, K.M., Shpikerman, V. V., Goryachev, N.A., Byalobzhesky, S.G., Frolov, Y.F., Khanchuck, A.I., Koch, R.D., Monger, J.W.H., Pozdeev, A.A., Rozenblum, I.S., Rodionov, S.M., Parfenov, L.M., Scotese, C.R., Sidorov, A.A., 2005. Metallogenesis and tectonics of the Russian Far East, Alaska and the Canadian Cordillera. In: U.S. Geological Survey, Professional Paper 1697 (397 p.).
O'Neill, J.M., Day, W.C., Aleinikoff, J.N., Saltus, R.W., 2010. The Black Mountain tectonic zone – A reactivated northeast-trending crustal shear zone in the Yukon-Tanana Upland of east-central Alaska. In: Gough, L.P., Day, W.C. (Eds.), Recent U.S. Geological Survey studies in the Tintina Gold Province, Alaska, United States, and Yukon, Canada—Results of a 5-Year Project: U.S. Geological Survey Scientific Investigations Report 2007–5289-D, 8p., Available at: https://pubs.usgs.gov/sir/2007/5289/SIR2007-5289-D.pdf (Accessed on 2/2020).
Page, R.A., Plafker, G., Pulpan, H., 1995. Block rotation in east-central Alaska: A framework for evaluating earthquake potential? Geology 23, 629–632. https://doi.org/10.1130/0091-7613(1995)023<0629:BRIECA>2.3.CO;2.
Phillips, J.D., 2002. Processing and interpretation of aeromagnetic data for the Santa Cruz Basin - Patagonia Mountains area, south-central Arizona. In: U.S. Geological Survey Open-File Report 298. http://pubs.er.usgs.gov/publication/ofr0298.
Piercey, S.J., Nelson, J.L., Colpron, M., Dusel-Bacon, C., Simard, R.-L., Roots, C.F., 2006. Paleozoic magmatism and crustal recycling along the ancient Pacific margin of North America, northern Cordillera. In: Colpron, M., Nelson, J.L. (Eds.), Paleozoic Evolution and Metallogeny of Pericratonic Terranes at the Ancient Pacific Margin of North America, Canadian and Alaskan Cordillera, Geological Association of Canada Special Paper 45, pp. 281–322.
Pilkington, M., Keating, P., 2006. The relationship between local wavenumber and analytic signal in magnetic interpretation. Geophysics 71. https://doi.org/10.1190/1.2163911.
Rasmussen, K.L., Lentz, D.R., Falck, H., Pattison, D.R.M., 2011. Felsic magmatic phases and the role of late-stage aplitic dykes in the formation of the world-class Cantung Tungsten skarn deposit, Northwest Territories, Canada. Ore Geol. Rev. 41, 75–111. https://doi.org/10.1016/j.oregeorev.2011.06.011.
Ray, G.E., 2013. A review of skarns in the Canadian Cordillera. In: British Columbia Ministry of Energy and Mines, British Columbia Geological Survey Open File 2013-08 (50p.).
Richter, D.H., Lanphere, M.A., Matson, N.A., 1975. Granitic plutonism and metamorphism, eastern Alaska Range, Alaska. Bull. Geol. Soc. Am. 86 (6), 819–829.

Saltus, R.W., Brown II, P.J., Morin, R.L., Hill, P.L., 2008. 2006 Compilation of Alaska gravity data and historical reports. In: U.S. Geological Survey Digital Series 264, CD-ROM. https://pubs.usgs.gov/ds/264/.

Sanchez, M.G., Allan, M.M., Hart, C.J.R., Mortensen, J.K., Zhang, R., Yalamanchili, R., Aitken, A., 2014. Extracting ore-deposit-controlling structures from aeromagnetic, gravimetric, topographic, and regional geologic data in western Yukon and eastern Alaska. Interpretation (Tulsa) 2, SJ75–SJ102.

Sawkins, F.J., 1984. Metal Deposits in Relation to Plate Tectonics. Springer, New York, N.Y. (325 p.).

Selby, D., Creaser, R.A., Hart, C.J.R., Rombach, C.S., Thompson, J.F.H., Smith, M.T., Bakke, A.A., Goldfarb, R.J., 2002. Absolute timing of sulfide and gold mineralization: a comparison of Re-Os molybdenite and Ar-Ar mica methods from the Tintina gold belt, Alaska. Geology 30, 791–794. https://doi.org/10.1130/0091-7613(2002)030<0791:ATOSAG>2.0.CO;2.

Shapiro, J., 2018. User's guide for MapMark4GUI—A graphical user interface for the MapMark4 R package. In: U.S. Geological Survey Techniques and Methods, book 7, chap. C18. https://doi.org/10.3133/tm7c18 (19p., accessed April 11, 2019, at).

Shapiro, J.L., Robinson, G.R., 2019. Resource Assessment Economic Filter (RAEF)—A graphical User Interface Supporting Implementation of Simple Engineering Mine Cost Analyses of Quantitative Mineral Resource Assessment Simulations. In: U.S. Geological Survey Techniques and Methods, book 7, chap. C23, 18 p.. https://doi.org/10.3133/tm7C23.

Sinclair, W.D., 1986. Molybdenum, tungsten and tin deposits and associated granitoid intrusions in the northern Canadian Cordillera and adjacent parts of Alaska. In: Morin, J.A. (Ed.), Mineral Deposits of Northern Cordillera: The Canadian Institute of Mining and Metallurgy, Special v. 37, pp. 216–233.

Singer, D., 1995. World class base and precious metal deposits – a quantitative analysis. Econ. Geol. 90, 88–104. https://doi.org/10.2113/gsecongeo.90.1.88.

Singer, D.A., Menzie, W.D., 2010. Quantitative Mineral Resource Assessments: An Integrated Approach: Oxford University Press (232 p.).

Soloviev, S.G., Kryazhev, S.G., Dvurechenskaya, S.S., 2020. Geology, mineralization, and fluid inclusion characteristics of the Agylki reduced tungsten (W-Cu-Au-Bi) skarn deposit, Verkhoyansk fold-and-thrust belt, eastern Siberia: Tungsten deposit in a gold-dominant metallogenic province. Ore Geol. Rev. 120, 103452.

Swanson, S.E., 1977. Relation of nucleation and crystal growth rate to the development of granitic textures. Am. Mineral. 62, 966–978.

Taylor, S.R., McLennan, S.M., 1985. The Continental Crust: Its Composition and Evolution: An Examination of the Geochemical Record Preserved in Sedimentary Rocks. Blackwell Scientific, Oxford (312 p.).

Thompson, K.M., 1978. Geology of the Clea Tungsten Deposit, Yukon Territory. Unpublished BSc Thesis. University or British Columbia (32 p.).

Thompson, J.F.H., Sillitoe, R.H., Baker, T., Lang, J.R., Mortensen, J.K., 1999. Intrusion-related gold deposits associated with tungsten-tin provinces. Mineral. Deposita 34, 323–334.

Tripp, R.B., Crim, W.B., Hoffman, J.D., O'Leary, R.M., Risoli, D.A., 1986. Mineralogical and geochemical naps showing the distribution of selected minerals and elements found in the minus-80-mesh stream-sediment and related minus-30-mesh heavy-mineral-concentrate samples from the Circle quadrangle, Alaska. In: U.S. Geological Survey Open-File Report 83–170 F (7 p).

Trop, J.M., Benowitz, J.A., Koepp, D.Q., Sunderlin, D., Brueseke, M.E., Layer, P.W., Fitzgerald, P.G., 2020. Stitch in the ditch: Nutzotin Mountains (Alaska) fluvial strata and a dike record ca. 117–114 Ma accretion of Wrangellia with western North America and initiation of the Totschunda fault. Geosphere 16 (1), 82–110. Available at. https://doi.org/10.1130/GES02127.1 (accessed on 10/7/2020).

U.S. Bureau of Mines, 1995. Final report of the mineral resource evaluation of the Bureau of Land Management Black River and Fortymile River subunits. In: U.S. Bureau of Mines Open-File Report 79-95 (229p.).

U.S. Geological Survey, 2020a. 5 Meter Alaska Digital Elevation Models (DEMs) – U.S. Geological Survey National Map 3DEP Downloadable Data Collection (accessed on 3/1/2020). https://data.usgs.gov/datacatalog/data/USGS:e250fffe-ed32-4627-a3e6-9474b6dc6f0b.

U.S. Geological Survey, 2020b. Mineral commodity summaries 2020. In: U.S. Geological Survey. https://doi.org/10.3133/mcs2020 (204 p.).

U.S. Geological Survey and U.S. Department of Agriculture, Natural Resources Conservation Service, 2013. Federal Standards and Procedures for the National Watershed Boundary Dataset (WBD) (4 Ed.): Techniques and Methods 11–A3 (63p.). https://pubs.usgs.gov/tm/11/a3/.

Union Carbide Corp. (UCC) Staff, 1979. Lucky 13 Project Area. Union Carbide Corporation (32 p.).

Wang, B., Case, G.N.D., Granitto, M., Labay, K.A., Shew, N.B., Ingraham, A.D., Bueghly, Z.C., Azain, J.S., Karl, S.M., Kelley, K.D., 2021. Data from the chemical analysis of archived stream-sediment samples, Alaska. In: U.S. Geological Survey Data Release. https://doi.org/10.5066/P9FR1D6Y.

Way, D., 1974. Geological report on the Morning Star Property (Oscar and Bailey claim groups, Yukon Territory). v.1, Canada Tungsten Mining Corporation, Frances Lake Area, Yukon. Yukon Mining Assessment Report 092120, 144 p. Available at: http://data.geology.gov.yk.ca/Reference/65701 (Accessed on: 10/7/2020).

Weber, F.R., Foster, H.L., Keith, T.E., Dusel-Bacon, C., 1978. Preliminary geologic map of the Big Delta quadrangle, Alaska. In: U.S. Geological Survey Open-File Report 78-529A. https://doi.org/10.3133/ofr78529A. Available at:. (Accessed 12/2/2020).

Wilson, F.H., Hults, C.P., Mull, C.G., Karl, S.M., comps, 2015. Geologic map of Alaska. In: U.S. Geological Survey Scientific Investigations Map 3340. https://doi.org/10.3133/sim3340 (pamphlet 196 p., 2 sheets, scale 1:1,584,000).